



# Fermi National Accelerator Laboratory

FERMILAB-Conf-83/75-EXP  
2000.000

## RECENT RESULTS ON D DECAYS AND LEPTON, PHOTON, (AND HADRON) PRODUCTION OF CHARM\*

Thomas Nash

September 1983

\*Invited rapporteur talk presented at 1983 International Symposium on Lepton and Photon Interactions at High Energies, Cornell University, Ithaca, New York, August 4-9, 1983.



RECENT RESULTS ON D DECAYS AND LEPTON,  
PHOTON, (AND HADRON) PRODUCTION OF CHARM

Thomas Nash

Fermi National Accelerator Laboratory  
P.O. Box 500  
Batavia, IL 60510 USA

INTRODUCTION

The study of charm production in lepton, photon and hadron beams involves severe experimental difficulties and large theoretical uncertainties. Progress, at least to those close to the subject, often appears excruciatingly slow. Why bother with such problems in an era of  $W^\pm$ ,  $Z^0$  and B production,  $\nu$  oscillations, and proton decay, all of which involve apparently cleaner and more comprehensible theory and experiment?

The answer and the motivation for this important subject lie in two directions. First and most straight forward is that the study of charm production allows the measurement of certain fundamental (and difficult) distributions such as the gluon structure function  $G(\eta)$ , the fraction of sea quarks that are strange, and the charm fragmentation function,  $D_C(Z)$ . Perhaps most important is that the study of charm production and decay is a major opportunity to develop an intuition into the workings of QCD. The large quark masses imply that  $\alpha_s = .2-.4$  and thus that the problem is in the domain of short distance QCD calculations. Clues from the experiments in this domain have an impact similar to early lattice gauge calculations in the QCD confinement realm. These results are leading to a developing understanding of how to calculate with what we all hope to be, finally, the theory of the strong interactions.

Perturbative QCD has had some successes and some difficulties in charm and hidden charm production. The successes have included the gluon fusion model prediction of distribution shapes in the  $q^2$ ,  $E_Y$ , and  $P_T$  variables in  $\mu$  and  $\gamma$  production. There have been difficulties involving absolute normalization. These manifest themselves as what must be called "fudge factors", the  $k$  factor of the Drell Yan process and the  $f$  factor from semi-local duality in gluon fusion predictions

of  $\psi$  elastic and inelastic cross sections. Charm decay measurement issues often involve the influence of the strong interactions on the weak decays of charm. Leptonic suppression, sextet dominance and the presence of non spectator diagrams are typical decay questions. These are discussed completely in Trilling's review.

The large acceptance and full reconstruction capabilities of the new generation of detectors in photon beams permits a detailed study of the hadronization of the  $c\bar{c}$  quark pair. The first such results, involving a measurement of the spectrum of masses emanating from the photon vertex accompanying the observed  $D^*$ , is reported at this conference. Hopefully, as more results like this are obtained theoretical effort will be brought to bear. The matter, it has been commented, is "...subject to rational thought, but hasn't (yet) been given any".<sup>2</sup>

The remainder of this review will take a primarily experimental view. The reader is encouraged to read the reviews with a theoretical emphasis on charm production and perturbative QCD by Halzen<sup>3</sup> at Paris and LePage<sup>4</sup> at this conference. Previous experimentally oriented reviews on subsets of our topic include Fisk<sup>5</sup>, Strovink<sup>6</sup> and Treille<sup>7</sup> at Bonn and Kalmus<sup>8</sup> at Paris. After a brief introduction to the experiments with results included in this review, we will discuss, in turn, production of  $\psi$  and  $\psi'$ , production of open charm in lepton and photon beams, D decays, and give a brief token mention of recent hadroproduction results. Emphasis will be on results reported since the Paris conference (August, 1982), but we will try to include all results since the last Lepton Photon Conference at Bonn (August, 1981) as well as earlier results when necessary for comparison.

#### Experiments Included In This Review

Lepton and photon experiments with results that were primarily reported in the period following the Bonn Conference but prior to last year's conference are:

CDHS	CERN - Dortmund - Heidelberg - Saclay CERN WA1 <sup>9</sup> $\nu(\bar{\nu}) \text{ Fe} \rightarrow \mu^{\pm} \mu^{\mp} X$
CCFR	Caltech - Columbia - Fermilab - Rochester - Rockefeller Fermilab E616 <sup>10</sup> $\nu(\bar{\nu}) \text{ Fe} \rightarrow \mu^{\pm} \mu^{\mp} X; \nu \text{ Fe} \rightarrow \mu^{\mp} \mu^{\mp} X$
$\nu$ -Emul.	Canada - Japan - US Fermilab E531 <sup>11</sup> $\nu + \text{Emulsion} \rightarrow \text{charm}$

BFP	Berkeley - Fermilab - Princeton Fermilab E203 <sup>12</sup> $\mu \text{ Fe} \rightarrow \psi X, 3\mu X$
EMC	European Muon Collaboration CERN NA2 <sup>13</sup> $\mu \text{ Fe} \rightarrow \psi X, 2\mu X, 3\mu X$
IF	Illinois - Fermilab Fermilab E401 <sup>14</sup> $\gamma p \rightarrow \psi' X$

In some cases final or updated results for these experiment have been made available during the last year. Drawings of each of these experiments are available in earlier publications or conference proceedings and will not be repeated here.

Three new hadron production experiments have recent results which will be mentioned briefly in the last section. These are shown in Figure 1 and are:

CERN Hyperon	Bristol-Geneve-Heidelberg-Lausanne-Rutherford CERN WA62 <sup>15</sup> $\Sigma^- \text{Be} \rightarrow A^+ (\text{csu})$
ACCMOR	Aachen-Bristol-CERN-Cracow-Munich-Rutherford CERN NA11 <sup>16</sup> $\pi \text{Be} \rightarrow D, D^*$
Fermilab Streamer Chamber	Yale-Fermilab-LBL Fermilab E630 <sup>17</sup> $n + \text{Streamer Chamber} \rightarrow \mu \text{ charm}$

An important dilepton result was made available at this conference:

Gargamelle	Bergen - CERN - Strasbourg Collaboration <sup>18</sup> $\nu_\mu N \rightarrow \mu^- e^- X$
------------	---

Three real photon experiments have new results on  $\psi$  and charm production:

SLAC Hybrid Facility $\gamma$ Collab.	Birmingham, Brown, Duke, Florida State, Imperial Coll., KEK, MIT, Nara Womens Univ., ORNL SLAC BC 72/73 <sup>19</sup> $\gamma p \rightarrow \text{charm}$
--	--

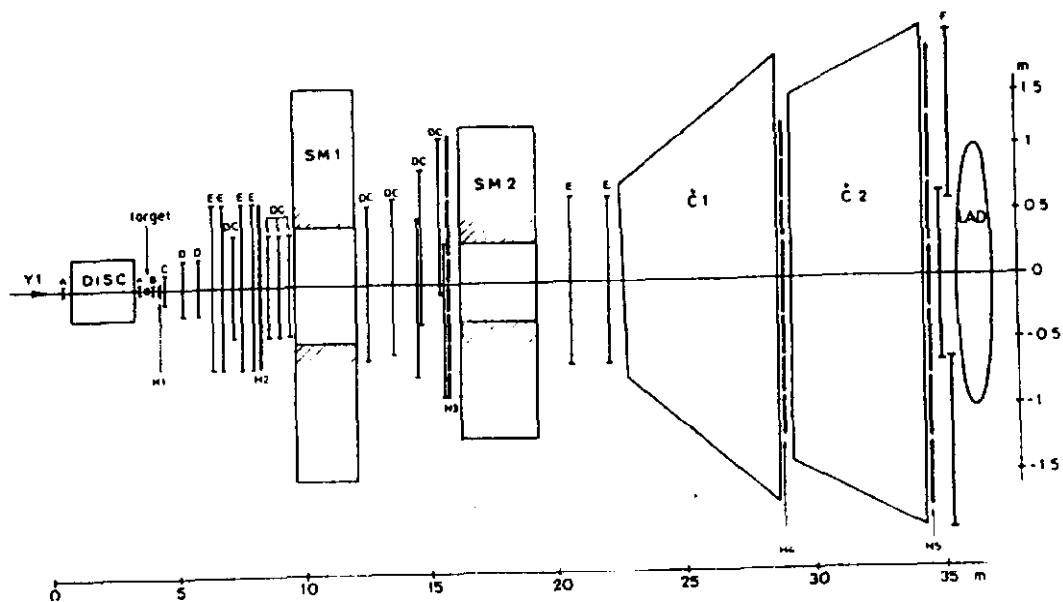


Figure 1a. CERN Hyperon Experiment.

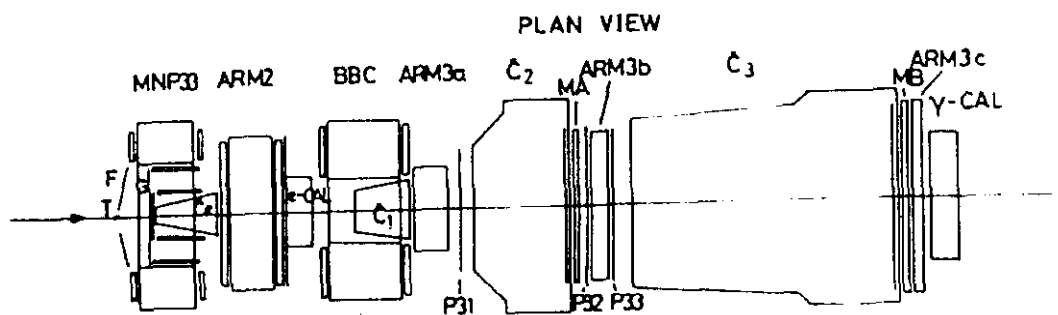


Figure 1b. ACCMOR Experiment.

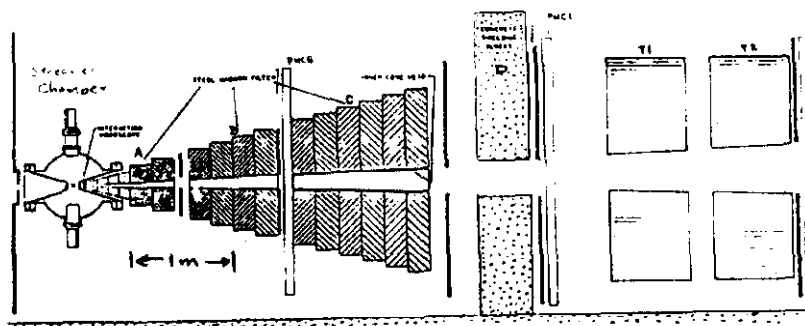


Figure 1c. Fermilab Streamer Chamber Experiment.

NA14	Athens, CERN, London, Orsay, Palaiseau, Paris, Saclay, Southampton, Strasbourg, Warsaw CERN NA14 <sup>20</sup> $\gamma\text{Li}^6 \rightarrow \psi X$
TPS(E516)	Carleton Univ., Fermilab, NRC, U.C. Santa Barbara, Univ. of Colorado, Univ. of Oklahoma, Univ. of Toronto Fermilab E516 <sup>21</sup> $\gamma p \rightarrow \psi X, D^* X p$

Figure 2 shows the SLAC Hybrid Facility and the Backscattered Laser Beam which allows a careful study of photoproduction mechanisms in a 20 GeV monoenergetic photon beam<sup>19</sup>. Charm decays are visible in the high resolution bubble chamber. Lifetime results from this experiment are reported in Reay's review at this conference.

The other two photon experiments are making their debut at this conference, reporting results for the first time. The NA14 experiment<sup>20</sup> uses an isotopic spin zero target ( $10\% X_0 \text{Li}^6$ ) because of planned QCD measurements. The detector (Figure 3) is located in a new high flux, yet tagged, photon beam and is intended to have a high level of sensitivity. The very large acceptance Goliath magnet is used as the main analysis magnet. Electromagnetic calorimeters and PWCs provide  $\pm 300$  mrad acceptance for photons and charged particles. Three segmented scintillator hodoscopes sandwiching  $\sim 4\text{m}$  of iron provide  $\mu$  identification over  $\pm 80$  mrad.

The Tagged Photon Spectrometer (TPS) is shown in Figure 4 and was first used by the Tagged Photon Collaboration for E516<sup>21</sup>. This large acceptance, charged and neutral, spectrometer with a sophisticated recoil detector is located in Fermilab's Tagged Photon Beam. The system has the potential for making a complete measurement of all 4-momenta of both the in state ( $\text{LH}_2$  target and tagged  $\gamma$  energy) and the out state (large acceptance recoil and forward measurement). This permits careful study of production mechanisms. The forward system includes 2 large acceptance magnets, 29 drift chamber planes, 2 segmented large volume Cerenkov counters for particle identification above 6 GeV, a high resolution segmented electromagnetic shower detector and a 300 ton hadron calorimeter and  $\mu$  scintillator wall. The recoil detector surrounds the  $\text{LH}_2$  target with 3 cylindrical MWPCs and 4 layers of  $dE/dX$  scintillators in 15 azimuthal sectors covering 94% of  $2\pi$ . This detector measures the angle and (for  $|t| < 1.2 \text{ GeV}^2$ ) the particle type ( $\pi$  vs  $p$ ) and energy of recoiling tracks. A high speed ECL-CAMAC trigger processor attached to the recoil system triggered on 2 types of recoil events: a) a single proton (from the primary vertex) recoiling off a forward "missing" mass,  $M_x > 2.5 \text{ GeV}$ ; b)  $\geq 3$  tracks recoiling from the primary vertex. The first trigger was intended to select elastic production and the second to enhance

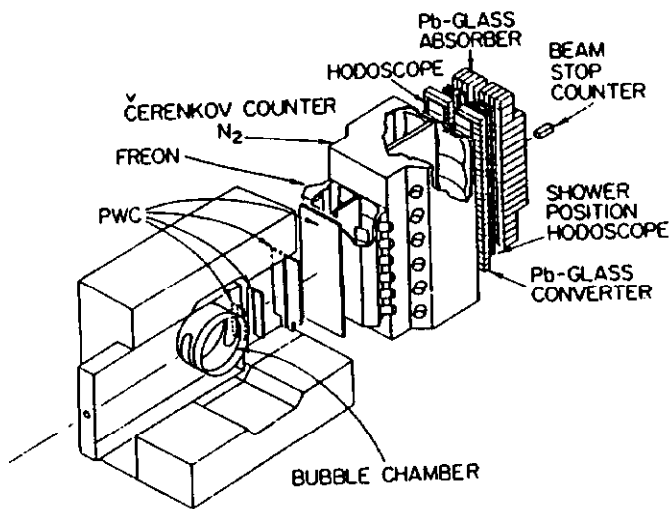


Figure 2  
SLAC Hybrid Facility  
and Backscattered  
Laser Beam.

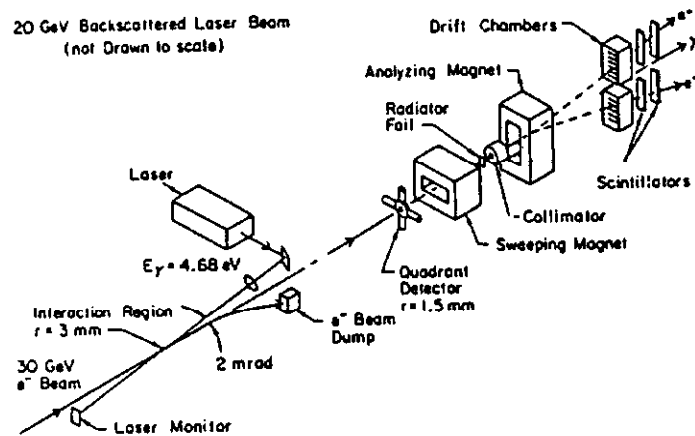
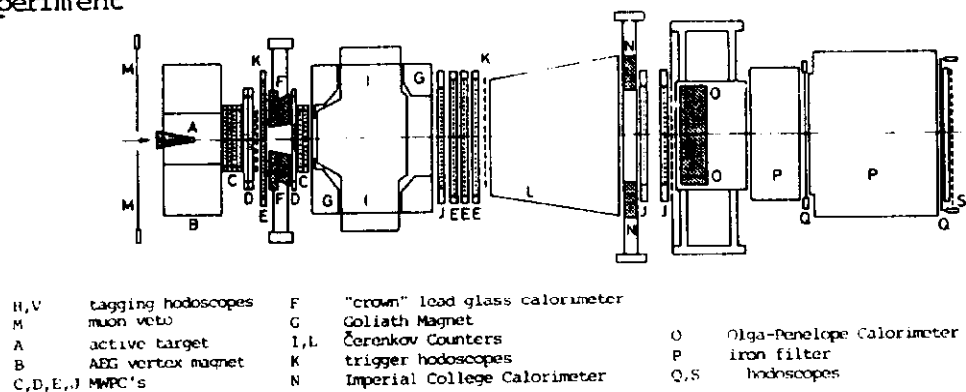


Figure 3.  
NA14 Experiment

NA-14

0 1 2 m



associated production ( $\Lambda$  recoil). In addition a di  $\mu$  trigger using the forward  $\mu$  wall was used for an unbiased study of  $\psi + 2\mu$  production mechanisms.

#### PRODUCTION OF $\psi$ AND $\psi'$

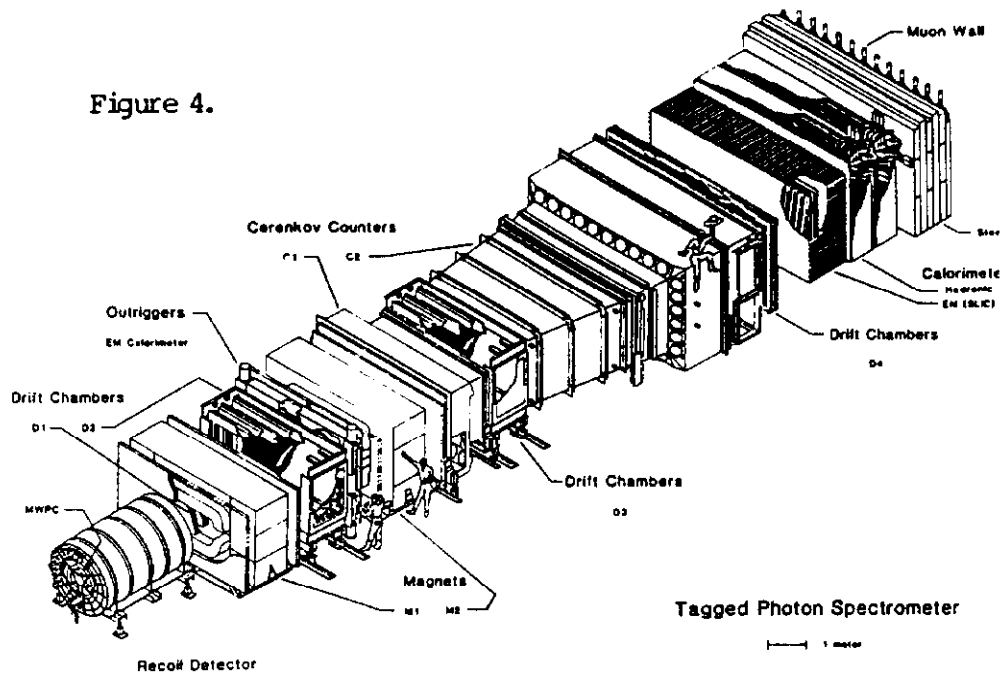
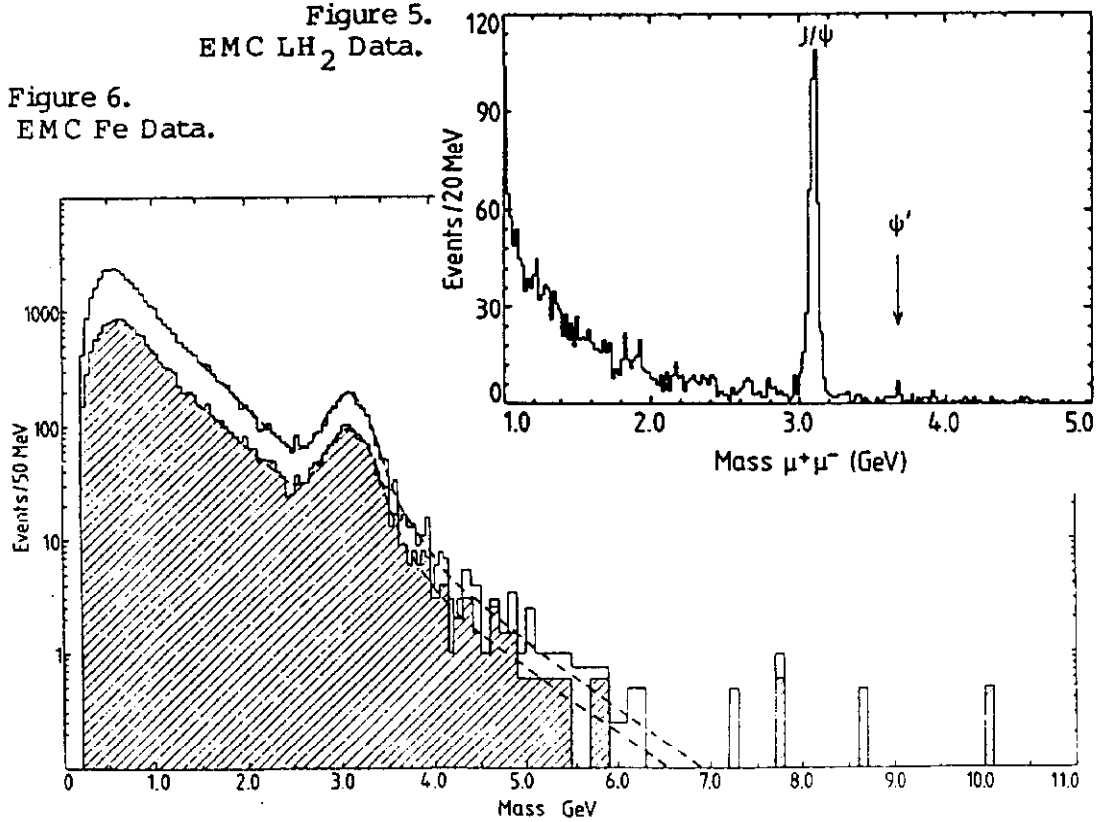
Strong signals for  $\psi$  photoproduction are now available from several  $\mu$  and photon experiments primarily in the  $\mu^+\mu^-$  channel. Figures 5-9 show the quality of recent data on  $\psi$  as well as indications for  $\psi'$  which, in most cases, have been used to measure the relative fraction  $\sigma(\gamma N \rightarrow \psi')/\sigma(\gamma N \rightarrow \psi)$ . Figure 10 shows a strong  $\psi' \rightarrow \psi \pi^+\pi^-$  signal observed by the Illinois-Fermilab group who also have a measurement of  $\psi' \rightarrow \mu^+\mu^-$ <sup>14</sup>. Their measurement of the  $\psi'/\psi$  fraction is the dominant one in the average obtained from the following list of results all of which are in agreement:

Experiment				$\frac{\sigma(\gamma N \rightarrow \psi' X)}{\sigma(\gamma N \rightarrow \psi X)}$	Ref.
E401	IF	$\psi' \rightarrow \psi \pi \pi$ $\rightarrow \mu \mu$	$\gamma p$	$0.20 \pm .05$	14
EMC-CERN		$\psi' \rightarrow \mu \mu$	$\gamma_{\nu} \text{Fe}$	$0.22 \pm .10$	13
EMC-CERN		$\psi' \rightarrow \mu \mu$	$\gamma_{\nu} p$	$0.22 \pm .12$	13
NA14-CERN		$\psi' \rightarrow \mu \mu$	$\gamma \text{Li}^6$	$0.24 \pm .10$	20
Average				$0.21 \pm .04$	

Elastic and inelastic  $\psi$  events have traditionally been identified by theorists<sup>22</sup> and the  $\mu$  experiments (BFP<sup>12</sup> and EMC<sup>13</sup>) on the basis of the fraction of the photon energy carried by the  $\psi$ ,  $Z = E_{\psi}/E_{\gamma}$ . In practice, events with  $Z > .9$  or  $.95$  (based on a hadron calorimeter measurement) have been called elastic, and events with  $Z < .9$  or  $.95$  called inelastic. Prior to 1983, as can be seen in Table I, there was an apparent discrepancy between the measurements of the ratio of  $\sigma_{\psi}^{\text{inelastic}}/\sigma_{\psi}^{\text{elastic}}$  by the  $\mu$  experiments (EMC and BFP) and that of the only real photon experiment then available (E401, Illinois-Fermilab)<sup>14</sup>. This difference, however, was not significant because the definitions of elastic and inelastic used by the photon experiment were completely different from the  $\mu$  experiments. For E401, essentially only inelasticity in the recoil region was considered since it was required that there be exactly two forward tracks, those of the  $\psi$ , for both elastic and inelastic events. Table I includes a brief summary of the definitions used by each



Figure 4.

Figure 5.  
EMC  $\text{LH}_2$  Data.Figure 6.  
EMC Fe Data.

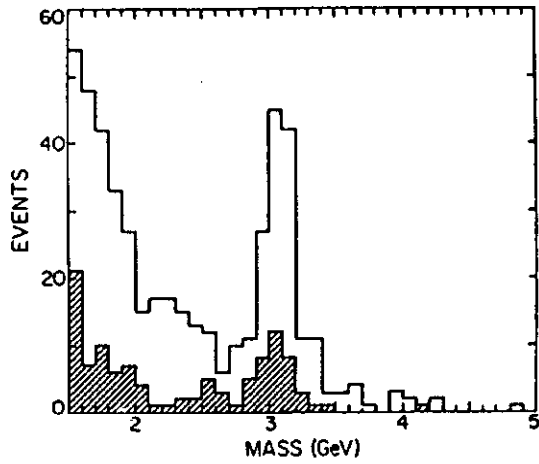


Figure 7. TPS dimuon mass spectrum.  
Shaded is inelastic data.

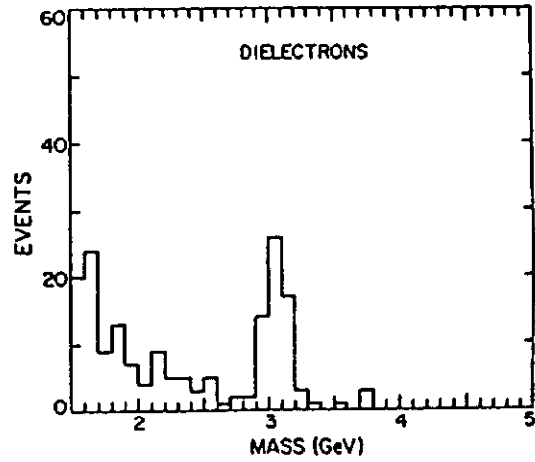


Figure 8. TPS dielectron mass spectrum.

Figure 9. NA14 dimuon mass spectrum. Figure 10. Illinois-Fermilab data.

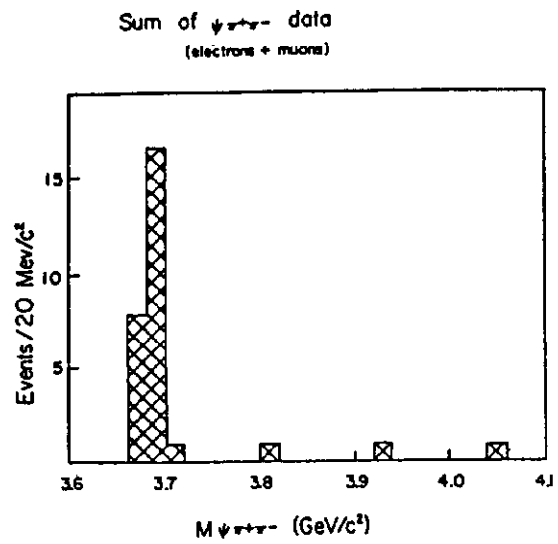
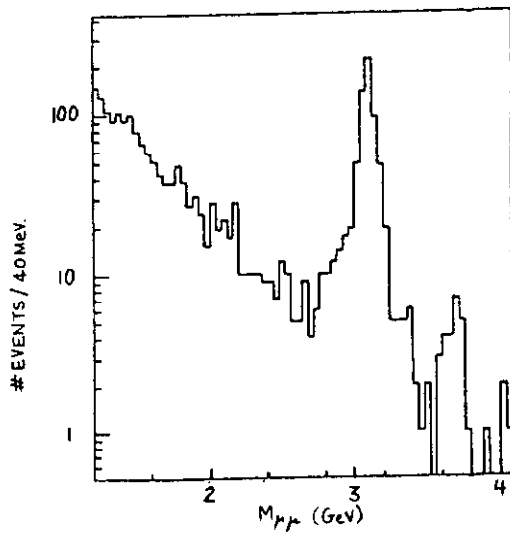


Table I.

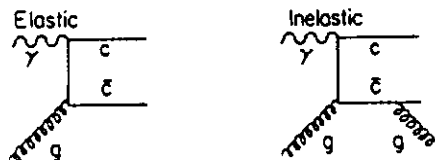
Elastic and Inelastic Photoproduction of  $\psi$  at  $\langle E_\gamma \rangle = 100$  GeV

Experiment	Ref	Definitions	$\psi$		$\psi$	
		Inelastic	Elastic	$\sigma_{\text{inelastic}}$ (nb)	$\sigma_{\text{elastic}}$ (nb)	$\frac{\sigma_{\text{inelastic}}}{\sigma_{\text{elastic}}}$
BFP $Q^2 \rightarrow 0$ 1980	$\mu\text{Fe}$ 12	Z<0.9	Z>0.95 ( $E_{\text{CAL}} < 4.5$ GeV)	$15.5 \pm 0.7 \pm 3.1$	$19.5 \pm 0.7 \pm 2.9$	$0.79 \pm 0.05$
EMC $Q^2 \rightarrow 0$ 1982	$\mu\text{Fe}$ 13	Z<0.95	Z>0.95	$20.6 \pm 1.8$	$12.9 \pm 1.1$	$1.6 \pm 0.2$
TPS E516 1983	Yp 21	Z<0.9 & recoil inel or extra fwd trks	Z>0.9 no extra fwd trks	$6.6 \pm 1.7 \pm 1.6$	$14.2 \pm 1.9 \pm 3.5$	$0.46 \pm 0.10$
NAL4 1983	$\gamma\text{Li}^6$ 20	extra tracks	no extra trks	$9.4 \pm 4.5 \pm 2.2$	$19.7 \pm 6.4 \pm 5.9$	$0.48 \pm 0.24$
IF E401 1982	Yp 14	2 fwd trks = $\psi$ recoil/fwd $\vec{p}$ imbal	2 fwd trks = $\psi$ $\vec{p}$ balance	$6.0 \pm 1.2 \pm 0.9$	$14.0 \pm 2.0 \pm 2.0$	$0.43 \pm 0.06$
TPS E516 1983	Yp 20	2 fwd trks = $\psi$ recoil/fwd $\vec{p}$ imbal	2 fwd trks = $\psi$ $\vec{p}$ balance	$4.4 \pm 1.3 \pm 1.1$	$9.8 \pm 2.0 \pm 2.5$	$0.45 \pm 0.12$
TPS E516 1983	Yp 20	Z<0.9 & recoil inel or extra trks - $\psi'$	fwd elastic	$5.1 \pm 1.7 \pm 1.2$	$14.2 \pm 1.9 \pm 3.5$	$0.36 \pm 0.08$
NAL4 1983	$\gamma\text{Li}^6$ 21	extra fwd or recoil trks - $\psi'$	fwd elastic	$7.3 \pm 3.5 \pm 2.2$	$19.7 \pm 6.4 \pm 5.9$	$0.37 \pm 0.19$

Notes: For comparison, results averaged over approximately  $60 \leq E_\gamma \leq 150$  GeV.  
Some results derived from reported data.

experiment and, for comparison, averages results over points covering the approximate range  $60 < E_\gamma < 150$  GeV with  $\langle E_\gamma \rangle \approx 100$  GeV. Where known, both statistical and normalization systematic errors are given. The experimental importance of the ratio of inelastic to elastic production lies in the fact that for practical purposes the normalization errors cancel in the ratio.

Problems with theoretical expectations, on the other hand, were not based on matters of definition. The basic success of the gluon fusion process in  $Q^2$ ,  $Z$  and energy distributions was established by EMC and BFP and reviewed by Strovink<sup>6</sup> and Halzen<sup>3</sup>. As indicated in the relevant diagrams



an extra hard gluon, and therefore an extra  $\alpha_s$ , is thought to be required to transfer sufficient energy to pass the inelasticity requirements. Thus, naively one expects

$$\sigma_{\psi}^{\text{inelastic}} / \sigma_{\psi}^{\text{elastic}} \approx \alpha_s \approx .3$$

which is hard to reconcile with the substantially higher values found by the EMC and BFP  $\mu$  experiments for this ratio as shown in Table I.

Most of the calculations of  $\psi$  cross sections have required a normalization factor,  $f$ , from semi-local duality<sup>23</sup> which assumes that the various charmonium channels share equally the available cross section below the  $D$  threshold. (This equal sharing is clearly inconsistent with the relative  $\psi' : \psi$  production ratio of  $.21 \pm .04$  discussed earlier.) An attempt to put gluon fusion normalization on a sounder footing (and at the same time answer fundamental complaints about this class of models by conserving color) was made by Berger and Jones<sup>24</sup>. Their "color singlet model" calculates an absolute cross section from the overlap of appropriate gluon fusion diagrams with a  $\psi$  wave function and the measured  $\Gamma_{ee}$  of the  $\psi$ . However, their first result, which used a natural value for the charm mass,  $m_c \approx 1/2 m_\psi \approx 1.5$  GeV and  $\alpha_s \approx .3$ , gave 4.5 nb for the inelastic cross section at 100 GeV. Since this was a factor of 3-5 below the  $\mu$  results (Table I), Baier and Ruckl<sup>24</sup> redid the calculation finding they could get good agreement with a very low  $m_c = 1.25$  GeV.

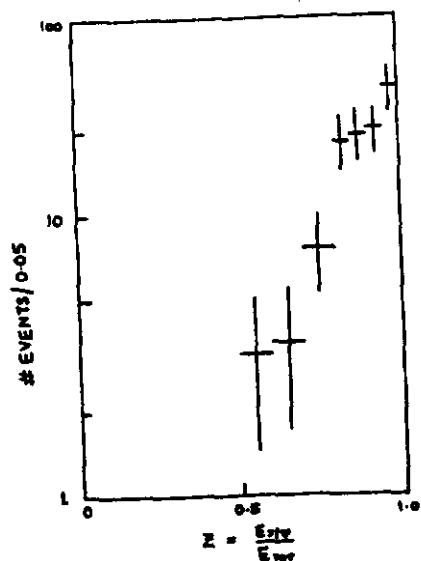
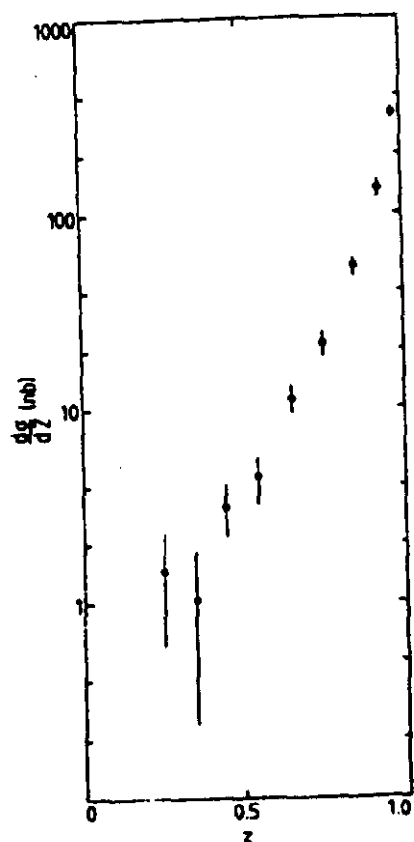
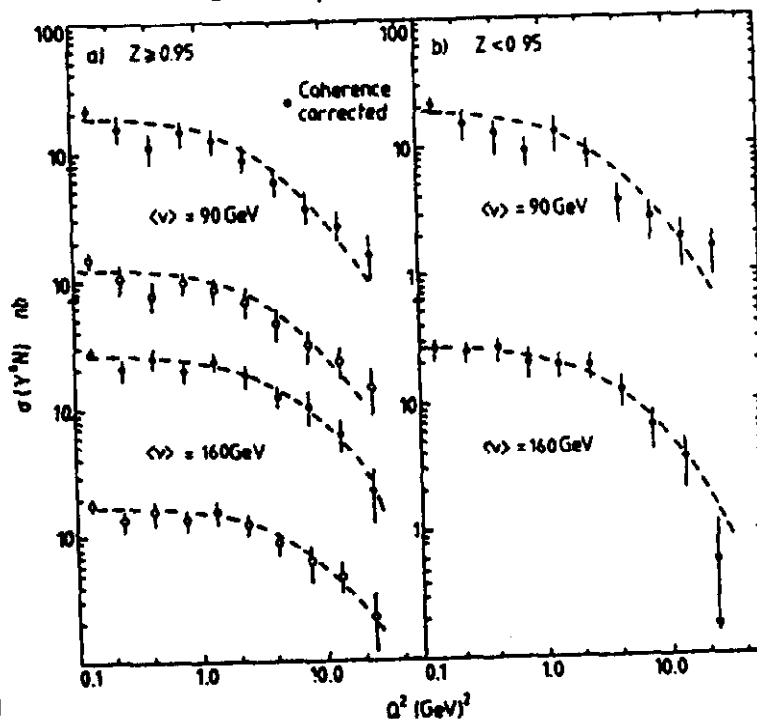
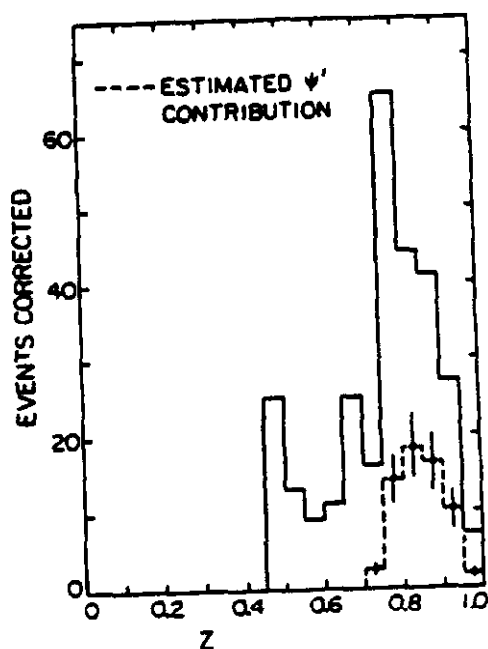
Two brand new results from photoproduction experiments were contributed to this conference and appear to clear up both the theoretical and experimental questions. Both new experiments (TPS-E516<sup>21</sup> and NA14<sup>20</sup> which agree with each other) can compare

directly with the muon experiments as shown in the top section of Table I. A clear disagreement between the new photon experiments and the muon experiments is seen both in the ratio and in the inelastic cross section. The TPS experiment with its full four momentum capabilities can also compare directly and finds itself in fine agreement with the recoil inelastic measurements of E401. Finally, taking advantage of the new measurement of the  $\psi'$  fraction the bottom section of Table I shows results for both new experiments with the  $\psi' + \psi$  background subtracted from the inelastic measurement. This gives the closest possible measurement of the theoretically calculated numbers. Figure 7 shows the inelastic signal in the TPS and Figure 11 shows the Z dependence and  $\psi'$  subtraction of TPS inelastic events. There is excellent agreement between the new photon experiments. They agree with the naive expectation for the inelastic/elastic ratio  $\approx \alpha_s \approx .3$  as well as with the original Berger-Jones calculation of the color singlet model using  $m_c = 1.5$  GeV.

Although the agreement with theory is very encouraging, the disagreement of the real photon experiments with the  $\mu$  results is hard to explain. The TPS results are on hydrogen, thereby eliminating in that experiment any possible nuclear effects from the use of Fe targets as was the case in the  $\mu$  experiments. Despite the fact that  $Li^6$  used by NA14 is closer to  $H_2$  than to Fe, the excellent agreement between NA14 and the TPS seems to rule out nuclear effects as an explanation of the discrepancy with the  $\mu$  experiments. The other major complication in the  $\mu$  experiments is the required  $Q^2$  extrapolation of  $Q^2$  to 0. Figure 12 shows typical examples of the  $Q^2$  fits used by EMC. There is no indication of any extrapolation problems that could explain the discrepancy. EMC's hydrogen data which has a good  $\psi$  signal (Figure 5) may provide another handle on what is going on here.

An example of some related distributions obtained by these experiments may be found in Figures 11-16. Figures 11, 13, 14 show the Z dependence. As theoretically expected the  $P_T$  distribution for inelastic events appears wider than for elastic events in the EMC data (Figure 15). TPS measures  $\langle P_T \rangle = 0.39 \pm 0.03$  for elastic and  $\langle P_T \rangle = 0.96 \pm 0.11$  for inelastic events. Finally, Figure 16 shows all the  $\mu$  and new photoproduction results ( $\psi'$  not subtracted) as a function of energy along with gluon fusion calculations. For most points only statistical errors are shown. However, in a few cases an extra error bar corresponding to systematic normalization errors is given so the significance of comparisons can be seen.

Both BFP and EMC have measured distributions in various azimuthal angles relevant in muonproduction. The BFP results and the angle definitions were discussed in detail by Strovink<sup>6</sup> at Bonn. Their conclusion is that a significant observed dependence on the angle  $\phi_F = \phi_{\text{decay}} - \phi_{\text{production}}$  saturates the expectations of s channel helicity conservation. For the record, we note that EMC results<sup>13</sup> find no

Figure 14. NA14:  $\psi$  vs  $Q^2$ .Figure 13. EMC:  $\psi$  vs  $z$ .Figure 12. EMC:  $\psi$  vs  $Q^2$  extrapolation  
fits to  $(1 + Q^2/M^2)^{-2}$ .Figure 11. TPS:  $\psi$  vs  $z$ .

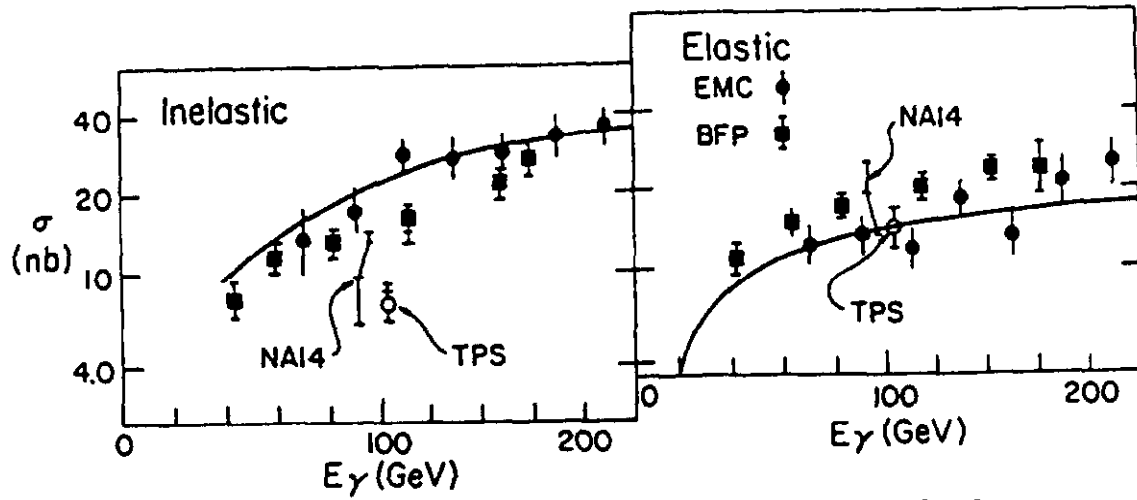


Figure 16. Summary of  $\psi$  data as a function of energy for elastic and inelastic events as defined by muon experiments (coherence corrected;  $\psi'$  not subtracted). See Table I.

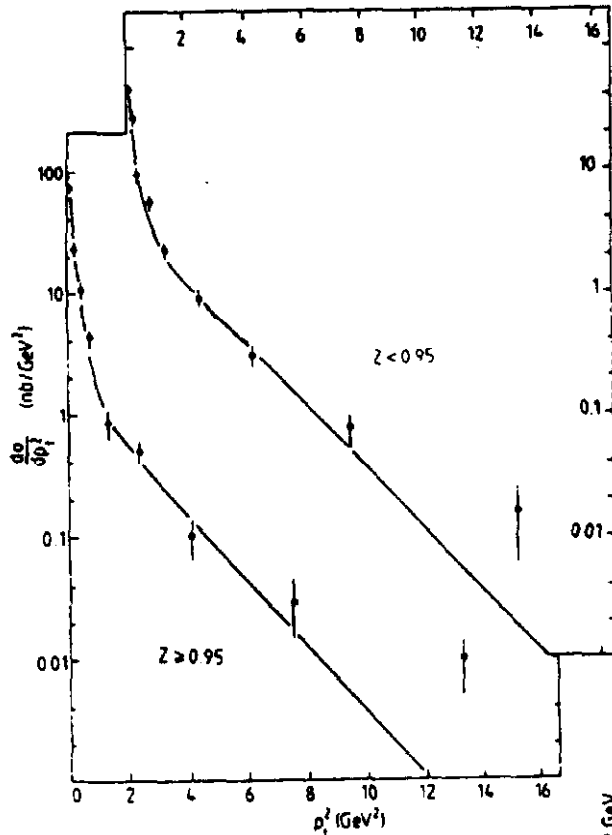
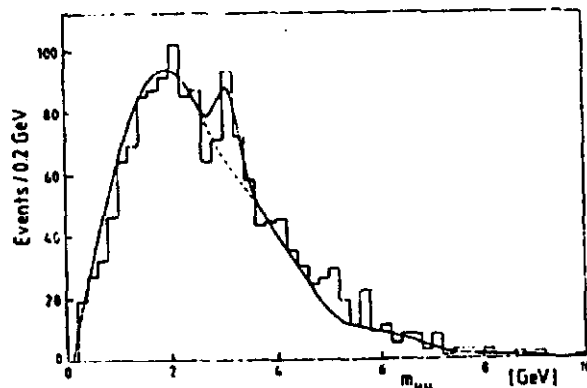


Figure 15. EMC  $\psi$  vs  $P_T$ . Curves are fits to sum of two exponentials.

Figure 17. CDHS: Neutrino neutral current dimuon spectrum.



significant  $s$  channel  $\phi_P$  dependence but do find a dependence on  $\cos\theta$  ( $\hat{p}_\psi \cdot \hat{p}_\gamma$ ) in the Gottfried-Jackson frame indicating the  $\psi$  is polarized along the virtual photon direction.

To conclude this section, Figure 17 shows the discovery by the CDHS group of neutral current  $\nu_\mu$  production of  $\psi + \mu^+ \mu^-$  with a cross section

$$\sigma_{\text{diffractive}}(\nu N \rightarrow \nu \psi X) = 4.2 \pm 1.5 \cdot 10^{-41} \text{ cm}^2/\text{nucleon}.^9$$

### PRODUCTION OF CHARM

There is much new data on real and virtual photoproduction of bare charm states which will be covered first in this chapter. The results include the energy,  $Q^2$ ,  $P_T$ ,  $t$ , and  $\theta^*$  distributions. A second subject will be clean information available for the first time on the question of how the  $c\bar{c}$  state hadronizes in terms of what accompanies the produced  $D$  or  $D^*$ . The third charm photoproduction topic to be discussed is the long standing debate on the relative amount of pair vs. associated production which has been clarified by a number of new results. The second section will summarize results from photon, muon, and neutrino experiments on the charm fragmentation function which complement the high energy  $e^+e^-$  fragmentation functions reviewed by Dorfan in these proceedings.<sup>31</sup> In the third section we will turn to neutrino production where charm production measurements have been used to determine the relative amount of strangeness among sea quarks. In closing we will summarize the continuing mystery of same sign dileptons produced in  $\nu$  experiments and the important question of what the source might and might not be. Charm as a source appears to be falling in the latter, might not, category.

### Charm: $\gamma$ , $\gamma_\nu$ Production

The muon experiments have been able to compare well measured distribution, such as  $E_\gamma$ ,  $P_T$ , and  $Q^2$ , with the gluon fusion model obtaining as a result the gluon structure function. These experiments have used di and tri muon final states from kinematic regions dominated by charm production and leptonic decay. Fully reconstructed charm states have only been seen in the real photon experiments. In these experiments the precise process observed is dependent on detector acceptance, trigger and analysis cuts. This is by way of warning that the cross section vs. energy summarized in Table II and Figure 18 must be compared with careful attention to the experimenters' definition of the process measured as cited in the table. (In this summary table and figure, older numbers have been adjusted for changes in relevant branching ratios in the Particle Data Tables.<sup>36</sup>)



Table II.

Summary of  $\gamma, \gamma_V$  N  $\rightarrow$  Charm Cross Sections

Experiment	Ref.	Process Measured	Energy Range (GeV)	$\langle E_\gamma \rangle$ (GeV)	$\sigma$ (nb)
CIF (E87)					
1979	25	$\gamma N \rightarrow D^0 \bar{D}^0$	50 - 200	$\sim 120$	$540 \pm 220$
1980		$\gamma N \rightarrow D^0 X$			$320 \pm 140$
		$\gamma N \rightarrow D^{*\pm} X$			$156 \pm 70$
1981		$\gamma N \rightarrow \Lambda_c^+ X$ [ $B(\Lambda_c \rightarrow Kp) = 1.5\%$ ]			$200 \pm 80$
$\Omega$ (WA4)					
1980	30	$\gamma p \rightarrow \bar{D}^0 X$	40 - 70	50	$570 \pm 190$
BFP					
1980	12	$\gamma_V N \rightarrow c\bar{c} X$ ( $E_{c\bar{c}}/E_\gamma$ large)		100	$560^{+200}_{-120}$
				178	$750^{+180}_{-130}$
EMC					
1982	13	$\gamma_V N \rightarrow c\bar{c} X$	60 - 100	80	$364 \pm 100 \pm 120$
			100 - 140	120	$535 \pm 62 \pm 144$
			140 - 180	160	$664 \pm 47 \pm 152$
			180 - 220	200	$715 \pm 40 \pm 150$

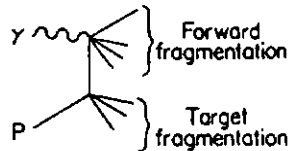
Table II. (cont.)

Experiment	Ref.	Process Measured	Energy Range (GeV)	$\langle E_\gamma \rangle$ (GeV)	$\sigma$ (nb)
SLAC Hybrid Y Collab. 1983	19	$\Upsilon p \rightarrow c\bar{c}X$ (observed decay)		20	$50^{+23}_{-19}$
TPS (E516) 1983		$\Upsilon p \rightarrow (D^{*+}X)p$ $\hookrightarrow D^0 \pi^-$ $D^0 \rightarrow K^- \pi^+$ $\rightarrow K^- \pi^- \pi^0$	40 - 160	100	$92 \pm 34$
					$88 \pm 21 \pm 26$ $103 \pm 33 \pm 35$
			40 - 80	60	$25^{+36+8}_{-25}$
			80 - 120	100	$103 \pm 32 \pm 33$
			120 - 160	140	$110 \pm 41 \pm 35$

Notes: Adjusted to latest Particle Data Book values  $B(D^{*0} \rightarrow K^- \pi^+) = 2.4 \pm 0.4\%$   
 $B(D^{*+} \rightarrow D^0 \pi^+) = 64 \pm 11\%^{36}$

Systematic errors (normalization and branching ratios) included in quadrature except when broken out for comparisons internal to one experiment.

The strong  $D^*$  signal observed in the  $-D^*-D$  mass difference spectrum in two  $D$  decay channels,  $K^+\pi^-$  and  $K^+\pi^-\pi^0$ , have allowed the E516 TPS group to make several new contributions to this conference regarding  $D^*$  production and decay.<sup>21</sup> Their combined data, background subtracted, is shown in Figure 20. With two different triggers (described in the introductory section) and careful offline analysis, this experiment can isolate certain subclasses of the total  $D^*$  cross section for measurement. Their  $(D^*x)p$  cross section cited in Table II and Figure 18 represents over half the  $D^*$  sampled and is limited to  $D^*x$  produced in the forward system accompanied by no more than a single proton from the primary vertex in the recoil system. In the lab the forward system covers about  $\pm 360$  mrad in the bend plane and  $\pm 72$  mrad in the non-bend plane. The recoil acceptance covers all production angles in the approximate range  $330 \text{ mrad} < \theta < \frac{\pi}{2} + 1000 \text{ mrad}$  for events with vertices at the upstream end of the target and  $1000 \text{ mrad} < \theta < \frac{\pi}{2} + 300 \text{ mrad}$  at the downstream end. In terms of pion rapidity in the lab frame the geometric acceptance for the recoil and forward systems is shown in Figure 21. In essence the recoil system covers completely the target fragmentation region near 0 rapidity which is 1-2 rapidity units wide, and the forward system covers the photon fragmentation region in the sense of the diagram:

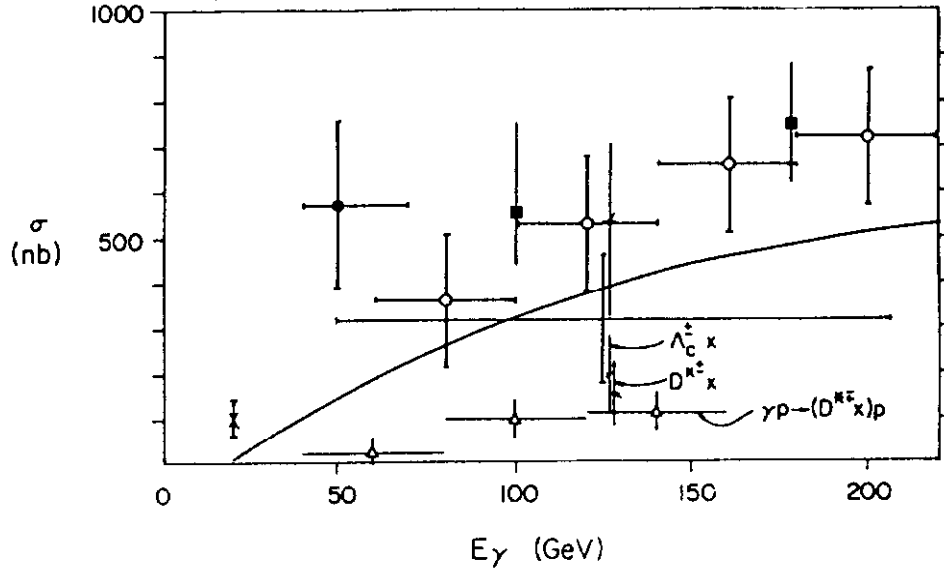


These definitions apply to all the subsequent results described from this experiment.

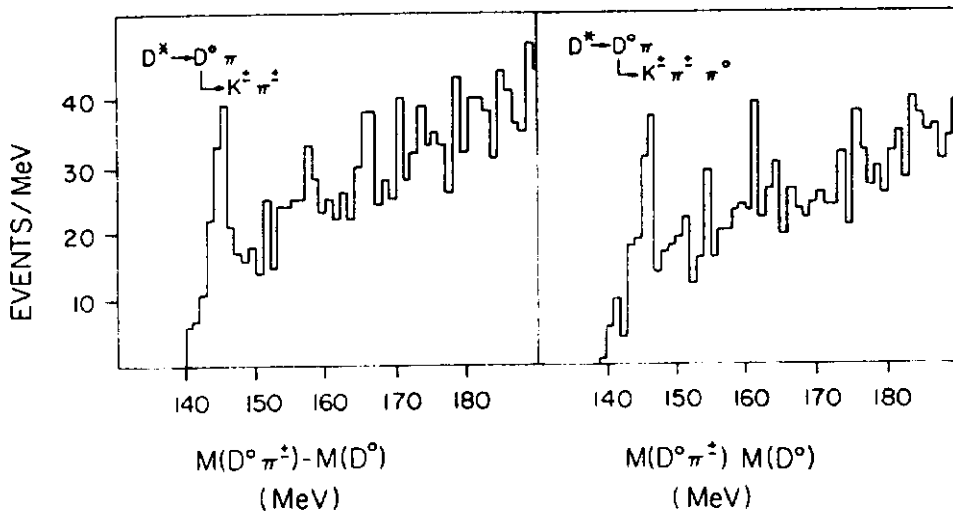
The TPS measurement of  $\sigma(\gamma p \rightarrow (D^*x)p)$  is of what is often loosely called the elastic or diffractive part of  $c\bar{c}$  production with  $c\bar{c} \rightarrow D^*x$ . This is in analogy to the semantics used in regard to photoproduction of vector mesons and is reinforced by the relatively sharp fall off in  $t$  shown in Figure 22 and the energy dependence which appears to be becoming relatively flat in Figure 18. This measurement is  $\sim 20\%$  of the total charm cross section (presumably dominated by  $D$  and  $D^*$ ) measured by EMC and BFP. The direct ratio of the TPS  $(D^*x)p$  and CIF  $D^*x^{25}$  measurement is

$$\frac{\sigma(D^*x p)}{\sigma(D^*x)} = .59 \pm .34$$

where errors are dominated by the relative normalization uncertainties. At the low end of the error range this ratio is 25% which is consistent with the general impression of  $\sim 20\%$  "elastic" production.



Measurements of large fractions of $\sigma_c$		Smaller parts of $\sigma_c$
$\oplus$ EMC $\gamma N \rightarrow c\bar{c} x$ $\mu$ Fe	$\dagger$ CIF $\gamma N \rightarrow D^0 \bar{D}^0 \gamma$ scintillator	$\dagger$ CIF $\gamma N \rightarrow \Lambda_c^+ x$ ( $\gamma$ scint.)
$\times$ SLAC Hybr. $\gamma$ FAC $\gamma p \rightarrow c\bar{c} x$ $\gamma p$	$\bullet$ $\Omega$ $\gamma p \rightarrow \bar{D}^0 x$ $\gamma p$	$\dagger$ CIF $\gamma N \rightarrow D^{*+} x$ ( $\gamma$ scint.)
$\oplus$ CIF $\gamma N \rightarrow D^{*0} x$ $\gamma$ Be	$\bullet$ BFP $\gamma N \rightarrow c\bar{c} x$ $\mu$ Fe "diffractive"	$\oplus$ TPS $\gamma p \rightarrow (D^{*+} x) p$

Figure 18. Summary of  $\sigma_c$  vs  $E_\gamma$ .Figure 19. TPS  $D^*-D$  mass difference histograms.

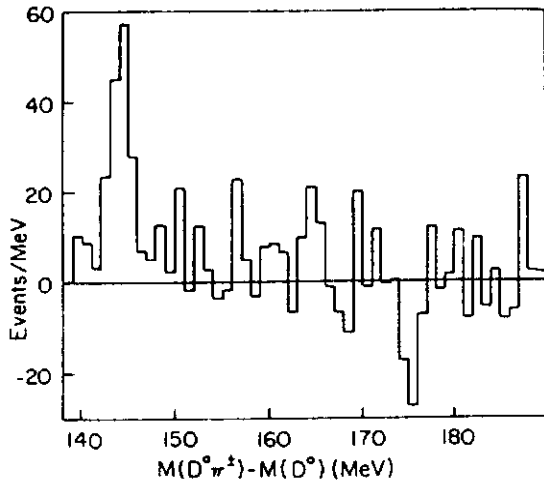


Figure 20. TPS background subtracted  $D^*-D$  mass difference,  $K\pi$  and  $K\pi\pi^0$  data combined.

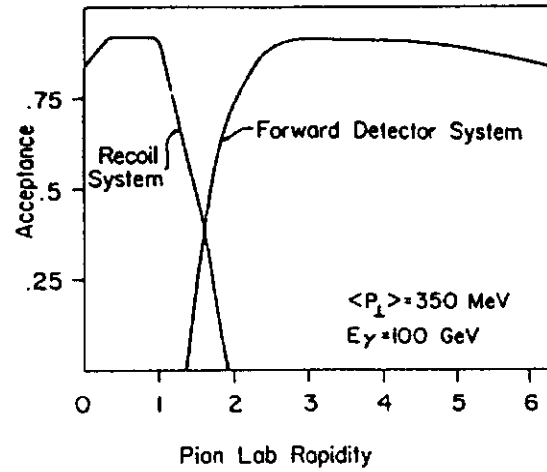


Figure 21. TPS lab rapidity acceptance for the recoil and forward detector systems. Calculated for pions assuming  $\langle P_T \rangle = 350 \text{ MeV}$ ,  $E_\gamma = 100 \text{ GeV}$ .

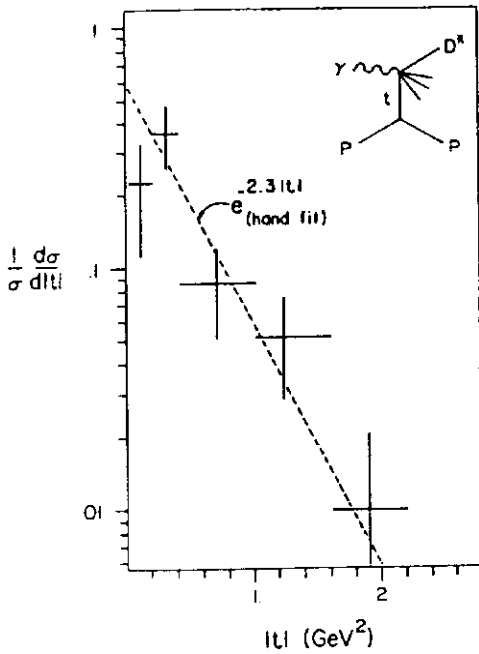


Figure 22. TPS  $t$  dependence for single proton recoil  $D^*$  data.

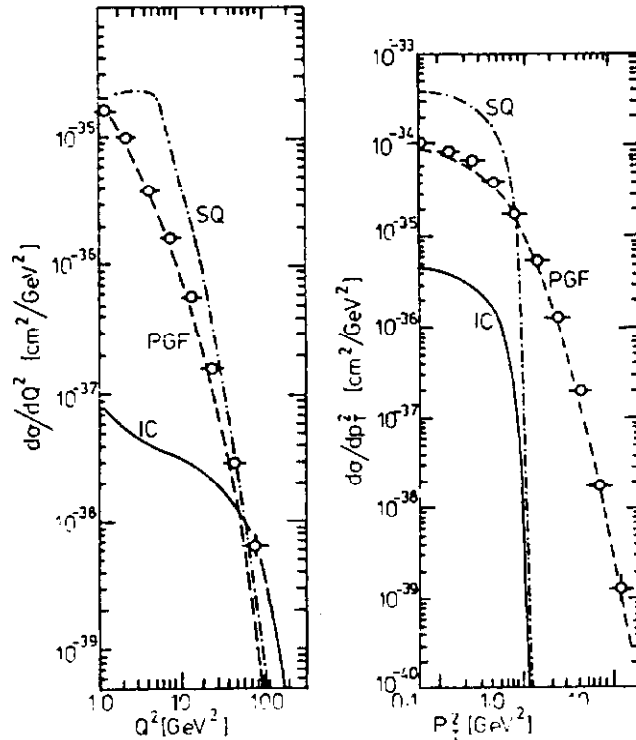


Figure 23. EMC  $Q^2$  and  $p_T^2$  dependence compared to photon gluon fusion (PGF), struck quark (SQ), and 1% intrinsic charm (IC) models.

The SLAC Hybrid  $\gamma$  Collaboration has provided an important new result tying down the open charm cross section at the low end of the energy scale in Figure 18. This low energy point is important (as Babcock, Sivers and Wolfram noted in 1978<sup>26</sup>) to gluon fusion determinations of the gluon structure function. The high  $\eta$  (fraction of momentum carried by the gluon) dependence of  $G(\eta)$  makes itself most conspicuous in its effect on the low energy turn on of the cross section. The "naive" form of the structure function

$$\eta G(\eta) = 3(1-\eta)^5$$

is expected from counting rule (high  $\eta$ ) and Regge theory (low  $\eta$ ) considerations. It allows the gluon fusion model to get good absolute agreement with  $P_T$  and  $Q^2$  distributions obtained by the  $\mu$  experiments as shown for the recent EMC results in Figure 23. Here the charm quark fragmentation function (see the next section)  $D_c(Z) = \exp(1.6Z)$  and quark mass,  $m_c = 1.5$  GeV, is used with the running coupling constant parameter  $\Lambda = .5$  GeV. A calculation<sup>26</sup> of the energy dependence of the  $\sigma_c$  using this "naive"  $G(\eta)$  is shown on Figure 18. Normalization issues aside, the new 20 GeV measurement by the SLAC Hybrid  $\gamma$  Collaboration suggests that a harder gluon distribution is required than the naive one. For example, the distribution<sup>27</sup>

$$\eta G(\eta) = 1.6(1-\eta)^7 + 12.6 \eta(1-\eta)^5$$

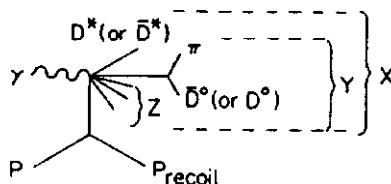
suggested by gluon bremsstrahlung calculations does a faster job of turning on the charm photoproduction cross section at low energy.

The single recoil proton  $D^*$  data of the TPS group has been used to study for the first time the angular distribution of the  $D^*$  in the center of mass of the photon fragmentation system - that is the c.m. of all particles except the recoiling proton<sup>21</sup>. The equivalent distribution in  $e^+e^-$  is flat in  $\cos\theta^*$ . Here, as suggested by Bjorken<sup>28</sup> in 1978, one expects forward-backward production to be enhanced because a backward going quark will be "wee" in the lab and therefore more readily interact with the target. Monte Carlo events with various  $\cos^{\eta}\theta^*$  distributions ( $\eta=0,2,4,6$ ) have been compared with histograms of the raw data in several variables. Two of these,  $P_T$  and  $\cos\theta^*$ , that are most sensitive to  $\eta$  are shown in Figure 24. Mean values for these two distributions for the data and the various values of  $\eta$  are:

	$\langle \cos\theta^* \rangle$	$\langle p_T^{D^*} \rangle$
data	.25	.75 GeV
flat M.C.	.08	1.44
$\cos^2\theta^*$ M.C.	.13	.99
$\cos^4\theta^*$ M.C.	.23	.80
$\cos^6\theta^*$ M.C.	.36	.65

Although likelihood fits have not yet been done, it appears that the best agreement will be for  $n \approx 4$  (or slightly larger). Thus, as expected,  $\theta^*$  peaks in the direction of the fragmenting photon system. Figure 25 shows the efficiency corrected TPS  $P_T$  distributions for single proton recoil as well as all  $D^*$  events.

Using their  $D^*$  data and almost complete coverage of the 4-momenta of the in and out going states, the TPS group has studied what accompanies the observed  $D^*$  as part of understanding how the  $c\bar{c}$  state hadronizes. Definitions are shown in the following diagram of the three groups of outgoing forward particles (X, Y, and Z) that can be measured to give information on the forward state with the  $D^*$ :



X represents all forward going particles, Y is the forward system except the observed  $D^*$ , and Z is the forward system exclusive of the observed  $D^{*+}$  and a presumed but not observed  $D^{*+}$ . Five essentially independent distributions (with varying sensitivity due to efficiency considerations) were measured. These are the masses of X, Y (two ways), and Z and the multiplicity of Y. All indicate that the  $D^{*+}$  is rarely accompanied solely by a  $D^{*+}$ .

The mass distribution,  $M_X$ , for single recoil proton events, determined as a missing mass from the in state photon and proton and out state recoil proton 4-momenta is shown in Figure 26. The turn on of  $D^*$  production is substantially higher than the  $D^*\bar{D}^*$  threshold suggesting the presence of additional particles. In Figure 27 is shown the raw observed multiplicity of charged tracks in Y, for all  $D^*$  events with no secondary interactions observed. This is compared to what is expected if  $Y=\bar{D}^*$  only by using SPEAR Mark II and Lead Glass Wall data<sup>1</sup> smeared by the TPS detection efficiency (dashed line histogram). The TPS  $n_Y$  distribution is clearly pushed to higher multiplicities than the  $Y=\bar{D}^*$  only shape. The mean  $Y=\bar{D}^*$  and observed multiplicities are  $\langle n_{\bar{D}^*} \rangle = 2.09 \pm 0.09$  and  $\langle n_Y \rangle = 3.20 \pm 0.26$ . The difference,  $\langle n_Y \rangle - \langle n_{\bar{D}^*} \rangle = 1.11 \pm 0.27$ , strongly indicates the presence on average of at least one additional particle.

The mass of the Y system, which should be 2 GeV for  $D^*\bar{D}^*$  only production, can be measured in two independent ways. The most sensitive measurement is made by calculating for single recoil proton events the missing mass,  $M_Y^R$ , of everything in the out state except the observed  $D^*$  and the recoiling proton. This distribution is shown in

Figure 24. TPS single proton recoil  $D^*$  raw events vs  $\cos \theta^*$  and  $P_T$ . Curves show Monte Carlo simulations for flat and  $\cos \theta^*$  CM dependence.

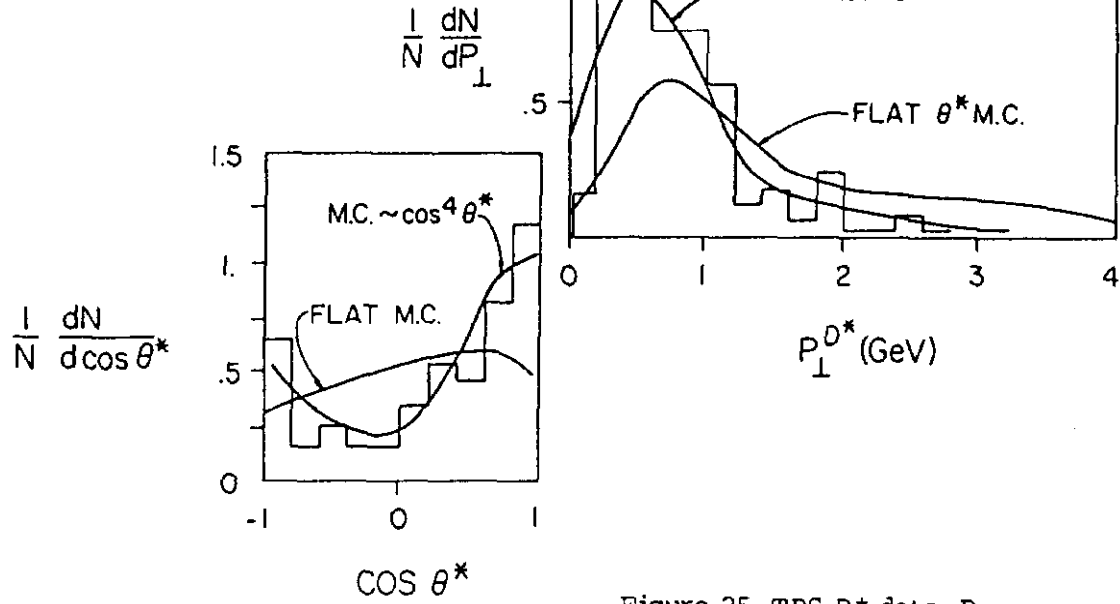


Figure 25. TPS  $D^*$  data:  $P_T$  dependence for single recoil proton sample and for all  $D^*$ s.

Figure 26. TPS single proton recoil  $D^*$  data sample:  $M_X$  dependence.

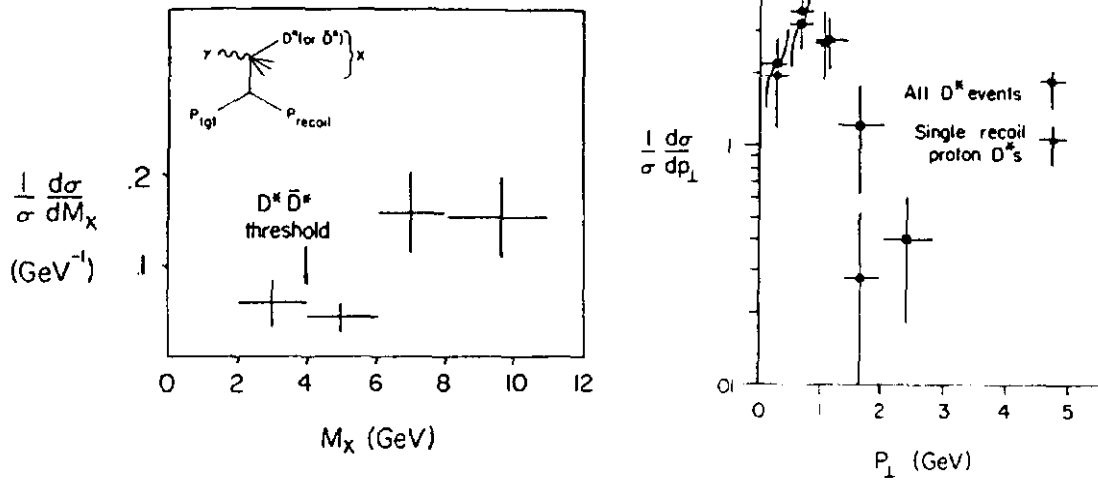




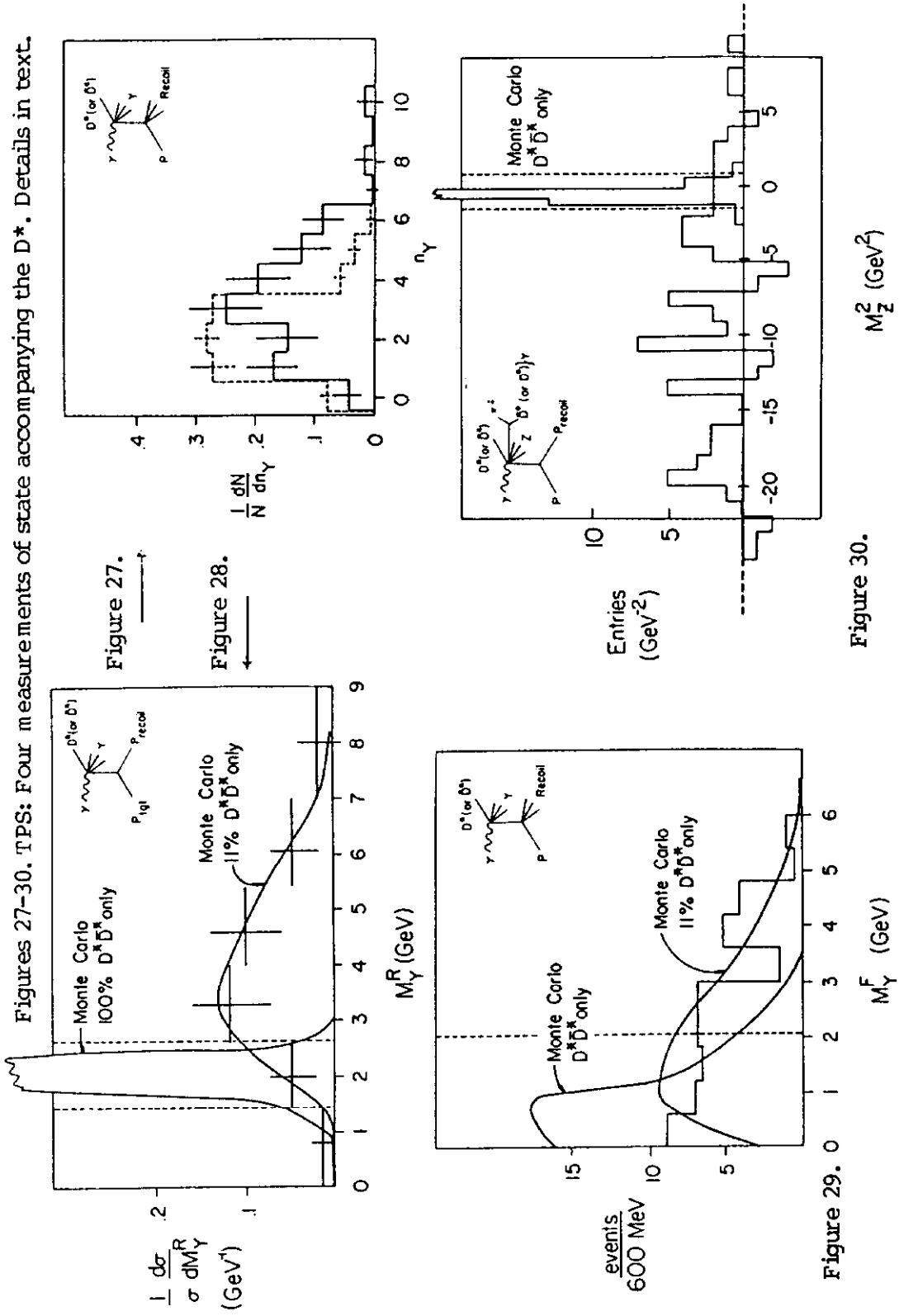
Figure 28. The dashed line  $\pm 600$  MeV around 2 GeV includes 95% of the Monte Carlo prediction of the distribution for  $D^*\bar{D}^*$  only events which peaks sharply at the  $D^*$  mass. Within this region falls only  $11 \pm 7\%$  of the data. This is the strongest indication of the relative rarity of  $D^*\bar{D}^*$  only production. The second curve shows the Monte Carlo expectation for 11%  $D^*\bar{D}^*$  only, 44.5%  $D^*\bar{D}^*\pi^+\pi^-$ , and 44.5%  $D^*\bar{D}^*\pi^+\pi^-\pi^0$ . Although this has excellent agreement with the data it is not intended to indicate that this distribution of extra particles is unique in matching the data. A second way of measuring the mass of Y is to compute  $M_Y^R$  directly from the observed particles (charged and neutral) in Y. This measurement shown in Figure 29 for all  $D^*$  events with no observed secondary interactions gives the same conclusion as  $M_Y^R$  but because of detection inefficiencies is much less sensitive and a poorer representation of the true  $M_Y$  distribution. Here the fraction below 2 GeV (where 92% of  $D^*\bar{D}^*$  only is contained) is  $47 \pm 18\%$ .

The fifth measurement in this study assumes the presence of a second  $D^*$  and computes  $M_Z$  of all particles in the forward system but the two  $D^*$ s. For  $D^*\bar{D}^*$  only production,  $M_Z = 0$ . The method is based on an observation by P. Avery<sup>25</sup> that since  $M_{D^*} - M_{D^0} - M_{\pi} = 5.9$  MeV is so small the 3-momentum of the  $D^*$  is, to a very good approximation, a constant times that of the  $\pi$ :  $\vec{P}_{D^*} \approx 14.36 \vec{P}_{\pi}$ . The 4-momentum of the  $D^*$  is then obtained by assuming the  $D^*$  mass.  $M_Z$  is computed for all available pions using the missing mass approach as for  $M_Y^R$  but here subtracting  $4P_{D^*}$  obtained in the manner just described. A small part of the resulting distribution in  $M_Z^C$  around zero is shown in Figure 30 with the Monte Carlo expectation for  $D^*\bar{D}^*$  only. The dotted line region contains 95% of Monte Carlo  $D^*\bar{D}^*$  only events and, at the 90% C.L. level,  $< 18\%$  of the data. Thus, in summary, all 5 measurements are consistent with the  $M_Y^R$  determination that only  $11 \pm 7\%$  of  $D^*$  are accompanied solely by  $\bar{D}^*$  and that the mass distribution of the extra particles accompanying the  $D^*$  continues smoothly to the kinematic limit.

The existence of associated photo production of charm ( $\gamma N \rightarrow \Lambda_c^+ D X$ ) is undeniable in view of the emulsion event published by the  $\Omega$  Photon-Emulsion Collaboration (WA58) in 1981<sup>29</sup>. Furthermore, associated production is remembered historically as having been an important mechanism in strangeness production. An important - and somewhat controversial - question for some time has been: how important is this mechanism in charm photoproduction?

The  $\Omega$  WA4 group came to the conclusion that  $\sigma(\Lambda_c^+ \bar{D} X) = 570 \pm 175$  nb which compared to  $\sigma(\bar{D} X) = 570 \pm 150$  nb suggests the dominance of associated production in their 20-70 GeV energy region. The errors allowed an upper limit  $\sigma(D^0 \bar{D}^0 X) < 445$  nb.<sup>30</sup> The conclusion was based on the presence ( $\sim 5\sigma$ ) of  $\bar{D}$  in the summed  $K^+\pi^-$  and  $K^+\pi^-\pi^0$  channels and the absence of  $D$  in the anti-channels. Furthermore, by requiring the additional presence of a p(or  $K^+$ ) identified by the Cerenkov detectors

Figures 27-30. TPS: Four measurements of state accompanying the  $D^*$ . Details in text.



the individual signals were enhanced to  $\sim 4\sigma$  and  $3\sigma$  respectively. The CIF data<sup>25</sup> at higher energy (50-200 GeV) supported opposite conclusions. Essentially equal numbers of  $\Lambda^+$  and  $\Lambda^-$  events were observed ( $27 \pm 8$  and  $26 \pm 7$  events respectively).<sup>c</sup> The ratio  $N_{D^{*+}}/N_{D^{*-}} = 1.4 \pm .4$  also favors dominantly pair production. Finally, requiring an additional opposite sign K(or p) enhanced the D signal as expected for pair production while requiring a same sign p(or K), the associated production signature, led to no signal.

The new information on this subject comes from three sources. EMC reports the ratio

$$R = \frac{\mu^+ \mu^- X}{\mu^+ \mu^+ X} = 1.13 \pm .10$$

in their charm sample for  $60 < E_\gamma < 220$  GeV. Any significant deviation from 1.0 in this ratio would represent a possible associated production contribution which is not indicated here. The TPS group for  $40 < E < 160$  GeV used a  $\Lambda_c$  sensitive recoil trigger (described in the introductory section) to look at  $R(\bar{D}^*/D^*)$ . They obtain the following upper limit:

$$\sigma(\gamma p \rightarrow \bar{D}^* \Lambda_c) < 60 \text{ nb (90\% C.L.)}.$$

They have no statement (yet) on  $\bar{D}^0 \Lambda_c$  production.

The most important new contribution on this matter comes from the SLAC Hybrid Facility  $\gamma$  Collaboration at  $E_\gamma = 20$  GeV. By a likelihood fit to the  $\bar{D}/D$  ratio, the number of detected  $\gamma \bar{D} D$  pair events, observed events with 2 charm decays, and the rate of  $K^0$  production they determine

$$\frac{\sigma(D\bar{D}X)}{\sigma(\text{charm})} = 65 \pm 20\%$$

The low energy and large acceptance of this experiment allow a direct comparison with WA4 in regard to whether associated production dominates in the threshold region.

Amplification of WA4's conclusion by earlier rapporteurs<sup>37</sup> may have given too strong an impression since the experiment (see discussion following this review) has been very careful to make clear that their results allow a sizeable cross section for pair production within the stated errors. Our most conservative conclusion on this matter at this stage is that pair production appears to be at least the majority of the cross section and that the large  $\sigma(\Lambda_c \bar{D}) \approx 500$  nb observed by WA4 remains unconfirmed.

### Charm Fragmentation Function

In principle the distribution of  $Z = E_{D^*} / E_c$  represents the charm quark fragmentation function,  $D_c(Z)$ . In practice, measurement and threshold issues complicate the situation. Despite this, there is excellent qualitative agreement among the fixed target measurements as well as with the  $e^+e^-$  results described in Dorfan's review.<sup>31</sup> A detailed comparison of  $e^+e^-$  and  $\nu$  results available before January of this year was made by Kleinknecht and Renk.<sup>32</sup> The  $Z$  threshold in a given reference frame is  $Z_{\text{threshold}} = M_{D^*} / E_{\text{quark}}$  and this imposes an artificial cutoff on direct measurements of  $D_c(Z)$  by fixed target experiments. Indirect measurements by  $\nu$  and  $\bar{\nu}$  experiments avoid the threshold problem but are complicated by fits and Monte Carlo calculations. Table III summarizes the measured quantities, the reference frames, and  $Z$  threshold for the various experiments with results on this subject.

The most direct fixed target measurement with a low threshold comes from the  $\nu$ -Emulsion experiment and is shown in Figure 31.<sup>11</sup> Another direct measurement, though with a high threshold, comes from the TPS group and is shown in Figure 32 for all single proton recoil data and for the subset with  $M_x > 6$  GeV that has a less severe threshold problem.<sup>21</sup>

EMC's indirect measurement of  $D_c(Z)$  is obtained from  $\mu^+Fe \rightarrow \mu^+\mu^-X$  and  $\mu^+\mu^-\mu^+X$  charm data. The result

$$D_c(Z) \sim e^{(1.6 \pm 1.6)Z}$$

in the lab frame<sup>13</sup> is similar to that of BFP<sup>14</sup>.

Neutrino experiments determine  $D_c(Z)$  from Monte Carlo fits to  $\nu(\bar{\nu})N \rightarrow \mu^+\mu^-X$  charm data. Although indirect, these measurements know the momentum transfer to the single charm quark and thus have less uncertainty than the  $\mu$  measurements. The best fit for  $D_c(Z)$  obtained by CDHS is shown in Figure 33.<sup>9</sup> The mean, but not the shape, is well determined by the fit since  $D_c(Z) = \delta(Z-.68)$  also fits well. CCFRR finds two satisfactory fits:

$$D_c(Z) \sim Z^A(1-Z)^B \quad (1)$$

with  $A = 0.5 \pm 1.5$  and  $B = 1^{+1}_{-.75}$  and

$$D_c(Z) \sim 1/[Z(1-1/Z-\epsilon/(1-Z))^2], \quad (2)$$

with  $\epsilon = 0.4^{+.25}_{-.11}$ . This form was suggested by Peterson<sup>32</sup> with the expectation that  $\epsilon \approx 1/(3 M_c^2)$ .

Table III

Experiments Measuring  $D_c(Z)$ 

Direct Measurements	Ref	Z	Frame	$Z_{\text{thresh.}}$
$\nu$ -Emulsion	11	$\frac{E_D(\Lambda)}{E_\nu - E_\mu}$	Breit	0.12
TPS $\gamma p \rightarrow X p^-$ $X \rightarrow D^{*+} (D^{*+} Y)$	21	$\frac{2E_{D^*}}{M_X}$	X CM	0.4
$e^+e^-$		$\frac{2E_D}{s}$	CM	0.13 PEP/PETRA 0.4 CLEO 0.5 SPEAR

Indirect Measurements	Ref	Measured "Z" for fit
$\mu^+Fe \rightarrow \mu^+\mu^-X$ EMC/BFP	13 12	$Z_m = \frac{E_{\mu \text{ decay}}}{\nu}$
$\mu^+\mu^-\mu^+X$ EMC	12	$Z_{\mu\mu} = \frac{E_{\mu 1} + E_{\mu 2}}{\nu}$
$\nu(\bar{\nu}) \rightarrow \mu^+\mu^-X$ CDHS CCFRR	9 10	$Z' = \frac{E_{\mu \text{ decay}}}{E_{\text{had}} + E_{\mu \text{ decay}}}$

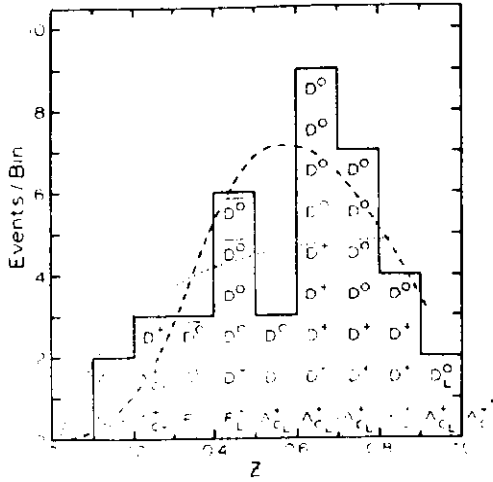


Figure 31. Neutrino-emulsion experiment:  $Z$  distribution of charm events.

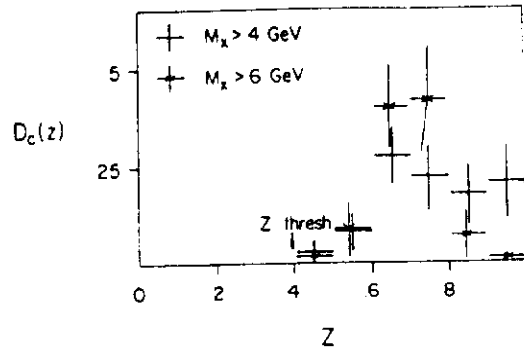


Figure 32. TPS single recoil proton data sample:  $Z$  distribution of  $D^*$  events for 2 cuts on missing mass,  $M_X$ , of forward particles.

Figure 33. Summary of charm fragmentation function data extracted from earlier experiments. (See Ref.36 and text.)

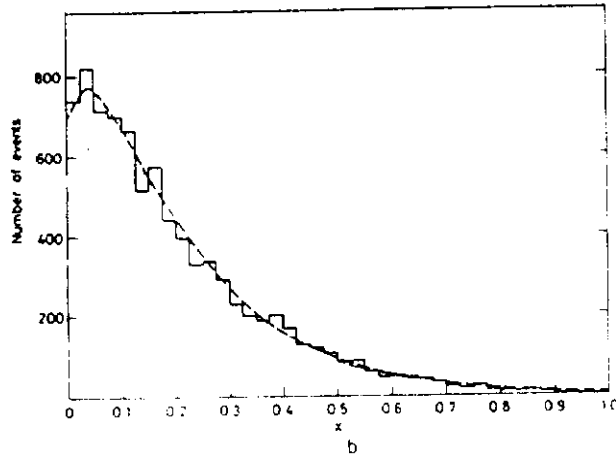
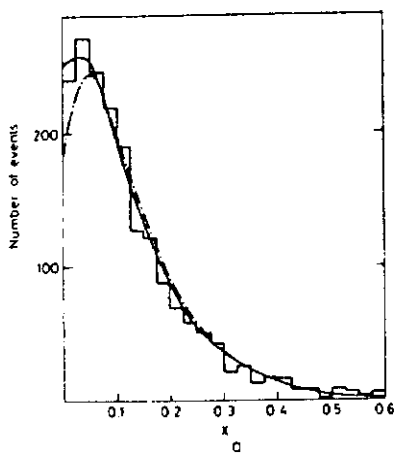
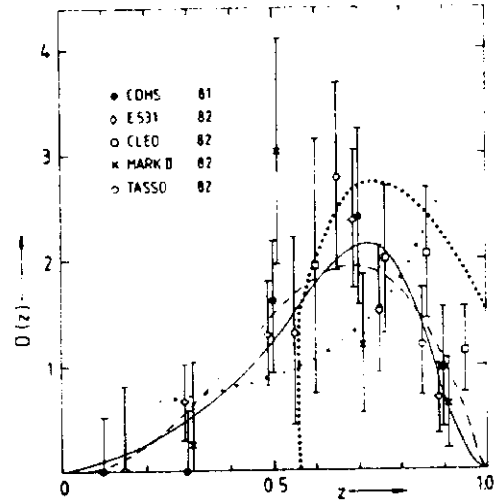


Figure 34. CDHS  $x_{vis}$  distributions: a) anti-neutrino; b) neutrino.

Figure 33 (from Ref. 32) summarizes the D(or D\*) fragmentation function extracted from earlier  $\nu$  and  $e^+e^-$  data. Here charmed baryons, with an apparently softer Z distribution, are removed from the  $\nu$ -Emulsion data. In this comparison to take into account different thresholds, appropriate normalization corrections have been made. Fits to the two forms of the fragmentation noted above are shown: (1) dashed line ( $A=2.8\pm.8$ ,  $B=1.3\pm.4$ ); (2) full line ( $\epsilon=.11\pm.04$ ). The dotted lines represent theoretical models cited in Ref. 32.

In sum, all experiments ( $\nu$ ,  $\gamma_\nu$ ,  $\gamma$ ,  $e^+e^-$ ) find a harder fragmentation function for charm than for light quarks. This is expected<sup>28</sup> since the inertia of the massive quark should be retained by the meson.

#### $\nu(\bar{\nu})$ Production of Charm: the Strange Sea

The difference between  $\nu$  and  $\bar{\nu}$  x distributions is immediately apparent from the CDHS data shown in Figure 34.<sup>9</sup> Although the same Feynman diagram is involved for both reactions, the x shape differs because  $\nu$  production, which goes as

$$d(x)u_{cd}^2 + s(x)u_{cs}^2,$$

is dominated by the valence d quark distribution, and the  $\bar{\nu}$  process,

$$\bar{d}(x)u_{cd}^2 + \bar{s}(x)u_{cd}^2,$$

involves only the narrower sea quark distributions. The relative fraction of the strange sea,

$$f = \frac{s}{\frac{1}{2}(\bar{u}+\bar{d})}$$

is determined by CDHS and CCFRR by essentially the same procedure:

- I. Determine shape of  $s(x) = \bar{s}(x)$  from  $\bar{\nu}$  distribution since  $u_{cd}$  is small. The resulting shape agrees with single  $\mu$  event determinations of  $\bar{u}$  and  $\bar{d}$ ;
- II. Fit  $\nu$  distribution to get the relative amount of strange sea,  $s(x)$ ;
- III. Use the charged current experiment measurements of  $\bar{u}$  and  $\bar{d}$  for the denominator of  $f$ .

(The CCFRR in addition uses the  $\bar{\nu}$  rate to get  $f$ .) The results for  $f$  are:

CDHS <sup>9</sup>	$0.52 \pm .09$
CCFRR <sup>10</sup>	$0.50^{+.16}_{-.18}$

These numbers agree with each other but appear to be substantially larger than similar  $e^+e^-$  measurements  $\sim .25-.3$  reported in Dorfan's review<sup>31</sup> from TPC and JADE. The significance of or reason for this apparent discrepancy is not clear.

Using similar procedures, CDHS and CCFRR also extract the K-M matrix element  $u_{cd} = \sin\theta_1 \cos\theta_2 = \sin\theta_c$  and the angle  $\theta_1$ . This is done assuming  $\sin\theta_1 = .228 \pm .011$ <sup>32</sup> and the average  $\nu$  produced charm semi-leptonic branching ratio,  $B_\mu = .071 \pm .013$ <sup>9</sup>. Their results:

	$u_{cd}$	$\cos\theta_1$
CDHS <sup>9</sup>	$.24 \pm .03$	$1.05 \pm .14$
CCFRR <sup>10</sup>	$.25 \pm .07$	$1.14 \pm .35$

The measurements of  $u_{cd}$  agree with the accepted value for  $\sin\theta_c = .230 \pm .003$  from strange decays.

#### $\nu$ Production of Charm: Like-sign Dileptons?

The  $\nu$ -emulsion experiment has measured directly the fraction of the charged current cross section corresponding to charm shown as a function of energy for  $\nu$  in Figure 35.<sup>11</sup> For  $\nu$  the average fraction for all charm is  $6.5^{+1.9}_{-1.8}\%$  and for  $D^0$  only it is  $2.5^{+.9}_{-.6}\%$ . For  $\bar{\nu}$  the average fraction is  $11^{+9}_{-5}\%$ .

This experiment has also obtained 90% C.L. upper limits (as fractions of the total  $\nu$ -charm cross section) of three possible sources of like sign dileptons. These are given in Table IV where we also show the resulting upper limits for  $\sigma(l^+l^-)/\sigma(l^-)$  the ratio usually given by experiments measuring the like sign effect. These are derived by using the fraction (6.5%) of charm obtained by this group and the  $\nu B_\mu = .071$  cited in the last section.<sup>9</sup>

In Figure 36 is shown roughly the range that includes all previous results (see Fisk's Bonn review<sup>5</sup>) as well as the final value of the CCFRR measurement, previously reported in preliminary form, and an important new result from Gargamelle.<sup>18</sup> The latter represents a rare  $\mu^-e^-$  measurement which has different systematic and background problems from the  $\mu^-\mu^-$  experiments. Here Dalitz pairs rather than  $K\mu$  and  $\pi\mu$  decays are the background. The cut on  $e^-$  momentum,  $P_{e^-} > 0.5$  GeV, is much lower than the typically 5-10 GeV calorimeter cuts in the  $\mu^-\mu^-$  experiments and probably explains why this point is relatively high.



Table IV

90% Upper Limits on Possible Sources of  $\nu$ -Like-sign Di Leptons<sup>11</sup>

Candidate Source		$\frac{\sigma(l^-l^-)}{\sigma(l^-)}$	$l=e \text{ or } \mu$
Charm pair production $\sigma(\mu c \bar{c} x)/\sigma(\mu c x)$	<6%	$<2.8 \cdot 10^{-4}$	
"Wrong sign" charm production $\sigma(\bar{c} \mu^- x) \sigma(c \mu^- x) + c \bar{c}$	<8%	$<3.7 \cdot 10^{-4}$	
Bottom production* $\sigma(b \mu X)/\sigma(c \mu X)$	<5%	$<2 \cdot 10^{-4}$	

\* $\tau \sim 10^{-12} - 10^{-13}$  sec

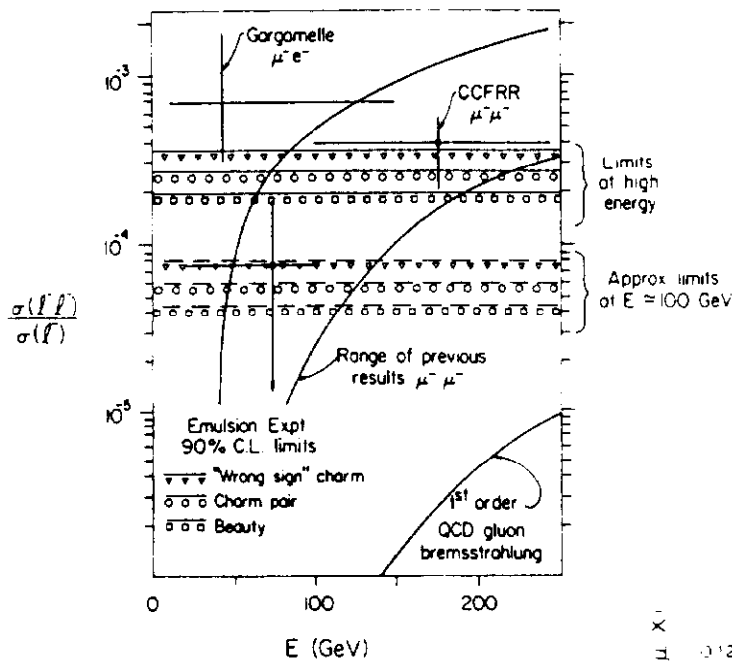
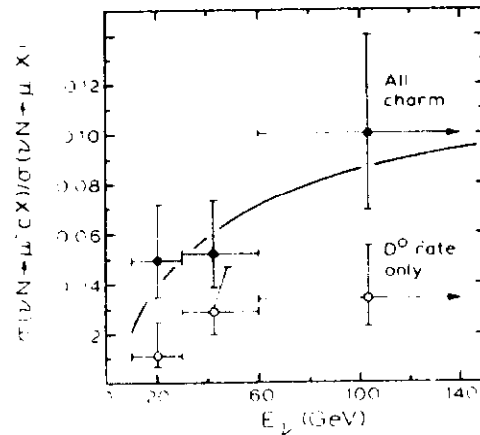
Figure 35. Neutrino-emulsion Experiment: neutrino production of total charm and  $D^0$  only vs energy.

Figure 36. Like sign di-leptons: recent results and approximate range of previous results. 90% C.L. limits from Neutrino-emulsion Experiment are shown. (See Table IV and text)



Also shown in Figure 36 is the typical first order QCD gluon bremsstrahlung calculation which is far too low. The limits on the three candidate sources from the  $\nu$ -emulsion experiments are shown in two ways. First, corresponding to high  $E_\nu$  where cuts on  $P_\nu$  do not affect efficiency, we show the limits as derived in Table IV.<sup>14</sup> Second, as an indication of how  $P_\nu$  cuts would reduce efficiency at low  $E_\nu$  to something like 20% of what it is at high  $E_\nu$ <sup>34</sup>, we show the limits multiplied by .2.

It is hard to draw a conclusion here. The data does not absolutely rule out the possibility of charm or bottom as sources. However, these explanations are becoming harder to support particularly in view of the fact that the Gargamelle experiment would expect 3-4  $V^0$ 's if  $c\bar{c}$  is the source, and they see none. Furthermore, no perturbative theoretical calculation comes close to predicting as much heavy quark production as is required to explain the data. Like sign di muons continue to be a serious mystery for the standard model.

#### D DECAYS

In this short chapter, we will cover recent results on D decays. S. Stone's review<sup>35</sup> discussed  $B_s$ , T, and F decays. The TPS group's strong  $D^*$  signals in the  $D^0 \rightarrow K^- \pi^+ \pi^0$  and  $K^- \pi^+$  (and c.c.) channels (Figure 19) allow them to measure the relative branching ratio with relatively little invocation of a Monte Carlo program. They have also been able to perform a detailed fit to the  $K^+ \pi^- \pi^0$  Dalitz plot to measure the branching ratios to resonant states.<sup>21</sup> In addition, there are several new branching ratios and limits determined by the ACCMOR group in channels with all charged final state particles.<sup>16</sup>

Using a carefully cleaned up sample of  $D^*$  with identical cuts in both channels, the TPS group measures

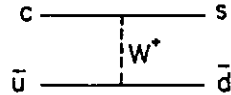
$$\frac{B(D^0 \rightarrow K^+ \pi^- \pi^0)}{B(D^0 \rightarrow K^+ \pi^-)} = 3.7 \pm 1.2 .$$

This ratio is relatively insensitive to detection efficiency of the charged K and  $\pi$  (subject to kinematic shifts readily modeled by Monte Carlo). The efficiency for reconstructing the  $\pi^0$  varies with energy from a threshold at 4 GeV to ~45% at  $\geq 30$  GeV and averages 28%. This was determined by adding to real events Monte Carlo generated photon showers and then processing the events by the usual  $\pi^0$  reconstruction program. The efficiency was checked by looking at the ratios of various  $K^*$  decays involving  $\pi^0$ 's and charged  $\pi$ 's. The  $K^*$  branching ratios are known absolutely from isotopic spin Clebsch - Gordon coefficients.

Multiplying the ratio given above by the Particle Data Booklet standard value<sup>36</sup> for  $B(D^0 \rightarrow K^+ \pi^-) = 2.4 \pm 1.4\%$  gives  $B(D^0 \rightarrow K^+ \pi^- \pi^0) = 8.9 \pm 3.2\%$  for the TPS measurement. Combining this with the Particle Table world average<sup>36</sup> of  $9.3 \pm 2.8\%$  gives a new world average

$$B(D^0 \rightarrow K^- \pi^+ \pi^0) = 9.1 \pm 2.1\% .$$

This data is also used for a study of the Dalitz plot (Figure 37). The study is motivated by the expectation of a significant contribution from the non-spectator W-exchange diagram in  $D^0$  decay



needed to explain the  $D^0$ - $D^+$  lifetime difference. This diagram has only  $I=1/2$  final states which leads to the relations:

$$\frac{B(D^0 \rightarrow K^- \pi^+)}{B(D^0 \rightarrow \bar{K}^0 \pi^0)} = \frac{B(D^0 \rightarrow K^{*-} \pi^+)}{B(D^0 \rightarrow \bar{K}^{*0} \pi^0)} = \frac{B(D^0 \rightarrow K^- \rho^+)}{B(D^0 \rightarrow \bar{K}^0 \rho^0)} = 2$$

(As Trilling notes<sup>1</sup>, a specific diagram is not required to reach this conclusion. Given Cabibbo favored decay modes and the  $|\Delta I|=1$  rule one can derive a triangular relation between relevant decay  $I$  spin pair amplitudes:

$$A(+-) + \sqrt{2} A(00) = A(0+) .$$

For a long  $D^+$  lifetime,  $A(0+) \rightarrow 0$ , and the ratios noted above follow.) Measurements of these decays by the Mark II experiment<sup>37</sup> gave values of  $1.36 \pm .73$  and  $1.64 \pm 1.01$  for the first two ratios, consistent with 2. However, the last ratio was inconsistent with 2 since  $B(K^- \rho^+) = 7.2 \pm 3.0$  and  $B(\bar{K}^0 \rho^0) = 0.1^{+0.6}_{-0.1}$ .

Both the  $D^0$  region and background region ( $D^0$  mass region, but outside  $D^*$  region) Dalitz plots (Figure 37a and b) are relatively smooth. In particular, in the background Dalitz plot the slow fall off in the horizontal axis,  $E_\pi$  decreases as  $M_{K-\pi}^2$  increases, indicates that the  $\pi^0$  efficiency is relatively good over the whole Dalitz plot.

The 82 events (of which 45% are background according to a fit) shown in Figure 44a represents the largest sample of  $D^0 \rightarrow K^- \pi^+ \pi^0$  yet collected. A maximum likelihood fit to this Dalitz plot yields the results shown in Table V along with the Mark II results.<sup>37</sup> The table gives the relative fraction of  $K^- \pi^+ \pi^0$  corresponding to each channel. Also shown are the branching ratios derived assuming the "new world average",  $B(K^- \pi^+ \pi^0) = 9.1 \pm 2.1\%$  cited earlier for the new TPS results. The Mark II branching ratios use  $B(K^- \pi^+ \pi^0) = 8.5 \pm 3.2\%$ .

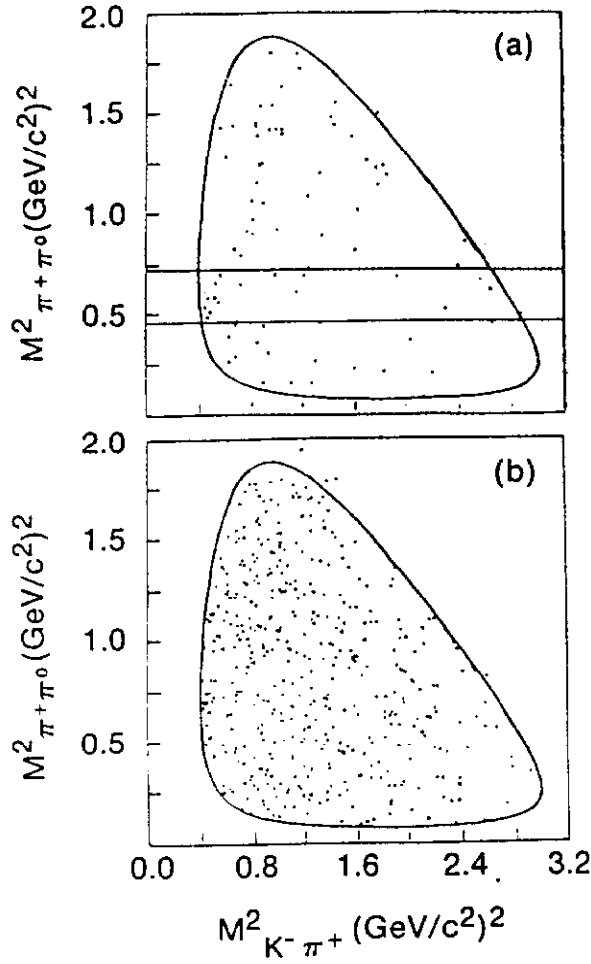


Figure 37. TPS:  $D^0 K^+ \pi^- \pi^0$  Dalitz plot. a)  $D^0$  region; b) background region:  $D^0$  mass, but not  $D^*$  mass.

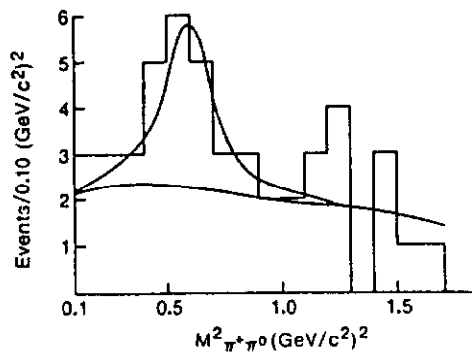


Figure 39. TPS: projection of Fig. 37a, for  $|\cos \theta| > 0.5$ .

Figure 38. Mark II:  $D^0 \rightarrow K^+ \pi^- \pi^0$  Dalitz plot.

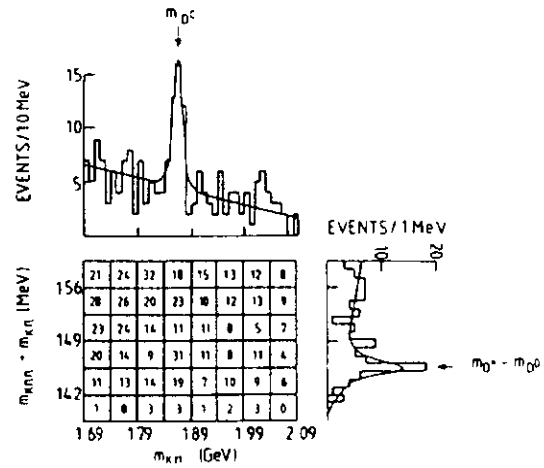
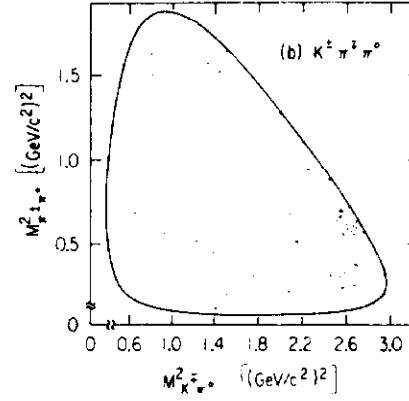


Figure 40. ACCMOR:  $m_{K \pi}$  vs  $(m_{K \pi \pi} - m_{K \pi})$  distribution; charged Ks and  $\pi$ s.

Table V  
Results of Fits to  $D^0 \rightarrow K^- \pi^+ \pi^0$  Dalitz Plot

Channel	Fraction		Branching Ratio (%)	
	TPS <sup>21</sup>	Mark II <sup>37</sup>	TPS <sup>21</sup>	Mark II <sup>37</sup>
$K^- \rho^+$	$0.31^{+.20}_{-.14}$	$0.85^{+.11}_{-.15}$	$2.8^{+1.9}_{-1.5}$	$7.2 \pm 3.0$
$K^* \pi^0$	$0.06^{+.09}_{-.06}$	$0.11^{+.14}_{-.09}$	$0.8^{+1.2}_{-0.8}$	$1.4^{+2.3}_{-1.4}$
$K^{*-} \pi^+$	$0.11^{+.12}_{-.08}$	$0.07^{+.07*}_{-.06}$	$2.9^{+3.3}_{-2.3}$	$3.4 \pm 1.4^*$
non-resonant	$0.50 \pm .23$	$0.00^{+.21}_{-.00}$	$4.5 \pm 3.0$	$0.0^{+1.9}_{-0.0}$

\*Average of fit to  $K^- \pi^+ \pi^0$   
and  $K^0 \pi^+ \pi^-$  Dalitz plots

The relatively low fraction of  $K^- \rho^+$  found in the TPS data is already evident by looking at the Dalitz plot (Figure 37a) on which the  $\rho$  band has been indicated.  $\rho$  events should cluster along the Dalitz plot boundary at the two ends of this band because of the  $\cos^2 \theta$   $\rho \rightarrow \pi\pi$  decay distribution. The Mark II Dalitz plot shown in Figure 38 (note the different horizontal axis from that used by TPS) has an apparent  $\rho$  cluster only at the end corresponding to high  $E_o$ . The other cluster would not have been detectable due to the fall off in  $\pi^0$  efficiency at low  $E_o$  for this  $e^+e^-$  experiment with its detection in the center of mass. The lack of a strong  $\rho$  effect in the TPS data is also evident if one looks at the one dimensional  $M_{\pi^+ \pi^0}^2$  histogram for events with  $|\cos \theta| > 0.5$  (Figure 39). Because of the  $\cos^2 \theta$  decay distribution, this cut removes  $\sim 1/2$  the background while keeping almost all of the  $\rho$ . The two curves show the result of the fit and the fit with  $\rho$  subtracted. Thus, even enhanced,  $\rho$  does not dominate this Dalitz plot.

Multiplying the TPS result by  $1/2$  gives

$$\frac{1}{2} B(D^0 \rightarrow K^- \rho^+) = 1.4^{+1.}_{-.8}$$

for comparison with <sup>37</sup>

$$B(D^0 \rightarrow \bar{K}^0 \rho^0) = 0.1^{+.6}_{-.1}.$$

This is now in approximate agreement ( $1.3\sigma$ ) with the expected ratio for a pure  $I = 1/2$  state (or for large  $\tau_D^+$ ). It is clear that a better measurement of the  $\bar{K}^0 \rho^0$  channel would be very desirable, and one hopes that this will be forthcoming soon from TPS, Mark III or ACCMOR.

The ACCMOR group also has a nice  $D^* - D$  sample (Figure 40) which they have obtained for  $D^0$  and  $D^\pm$  in  $\pi^- Be$  interactions.<sup>16</sup> With this data they are able to obtain a number of charged channel decay ratios which are given in Table VI.

In Table VII are listed derived values for the various  $D^0$  and  $D^\pm$  branching ratios, Particle Data group numbers<sup>36</sup> for comparison when available, and new weighted world averages. These use the Particle Data Group values<sup>36</sup>,  $B(D^0 \rightarrow \bar{K}^- \pi^+) = 2.4 \pm .4\%$  and  $B(D^+ \rightarrow \bar{K}^- \pi^+ \pi^+) = 4.6 \pm 1.1\%$ .

#### HADROPRODUCTION OF CHARM

The subject of hadroproduction of charm is not formally included among topics that fall within the domain of a "Lepton-photon" conference. Nonetheless, because of the close relationship to some of the matters included in this review, we will make a brief mention of recent hadroproduction results.

The D decay results from the ACCMOR experiment have already been discussed (see Figure 40 and Tables VI and VII). This group has also measured the cross section<sup>16</sup> assuming an  $A^1$  dependence

$$\sigma(\pi^- Be \rightarrow D \bar{D} X) = 48 \pm 15 \pm 24 \text{ } \mu\text{b/Nucleon}$$

at 175 and 200 GeV. To compare with results based on an  $A^{2/3}$  dependence assumption, this result should be multiplied by 2.1. Assuming  $A^1$ , the CCFRS beam dump experiment<sup>38</sup> measures the same cross section on Fe to be  $22.6 \pm 2.1 \pm 3.6 \text{ } \mu\text{b/nucleon}$ . This should be multiplied by 3.8 for  $A^{2/3}$ . The two experiments are in better agreement for the  $A^{2/3}$  assumption which gives  $101 \pm 31 \pm 50$  (ACCMOR) and  $86 \pm 4.4 \pm 7.6$  (CCFRS)  $\mu\text{b/nucleon}$ . In fact recent results from the E613 Fermilab, Firenze, Michigan, Ohio, Wisconsin beam dump experiment which used two different A targets indicates an  $A$  dependence similar to the total inelastic cross section  $A^{.72}$ .<sup>39</sup>

The ratio

$$\frac{\sigma(120 \text{ GeV})}{\sigma(175/200 \text{ GeV})} = 0.62 \pm .34$$

indicates ACCMOR may be seeing a rise as would be expected given the

Table VI

New ACCMOR Results on  $D^0$  and  $D^\pm$  Decays<sup>16</sup>

$\frac{D^0 \rightarrow K^+ \pi^- \pi^+ \pi^-}{D^0 \rightarrow K^+ \pi^\pm}$	$2.0 \pm 1.0$
$\frac{D^0 \rightarrow K^* \rho^0}{D^0 \rightarrow K^+ 3\pi^\pm}$	$0.5 \pm 0.2$
$\frac{D^0 \rightarrow K^+ \pi^- \rho^0}{D^0 \rightarrow K^+ 3\pi^\pm}$	$0.2 \pm 0.2$
$\frac{D^0 \rightarrow K^* \pi^\pm \pi^\mp}{D^0 \rightarrow K^+ 3\pi^\pm}$	$< .18$ (90% C.L.)
$\frac{D^\pm \rightarrow K^+ 4\pi^\pm}{D^\pm \rightarrow K^+ 2\pi^\pm}$	$< .16$
$\frac{D^\pm \rightarrow K^* \pi^\pm}{D^\pm \rightarrow K^+ 2\pi^\pm}$	$< .22$

Table VII

New  $D^0$  and  $D^\pm$  Branching Ratios

Channel	ACCMOR <sup>16</sup>	Branching Ratio Part. Data Book <sup>36</sup>	New World Average
$K^+ \pi^- \pi^+ \pi^-$	$4.8 \pm 2.5\%$	$4.5 \pm 1.3\%$	$4.6 \pm 1.2\%$
$K^* \rho^0$	$2.3 \pm 1.1\%$	---	$2.3 \pm 1.1\%$
$K^\pm \pi^\mp \rho^0$	$0.9 \pm 0.9\%$	---	$0.9 \pm 0.9\%$
$K^* \pi^\pm \pi^\mp$	$< .83\%$	---	$< .83\%$
$K^+ 4\pi^\pm$	$< .74\%$	$< 4. \%$	$< .74\%$
$K^* \pi^\pm$	$< 1.0\%$	$< 3.7\%$	$< 1.0 \%$

very high cross sections seen at the ISR. They also measure the  $P_T$  and  $x_F$  distribution

$$\frac{d^3\sigma}{dP_T^2 dx_F} \sim (1-x_F)^{0.8 \pm .4} e^{-(1.1 \pm .5)P_T^2}$$

This distribution rules out perturbative gluon fusion and quark annihilation models<sup>22</sup> which also predict a much lower cross section. However, flavor excitation models<sup>40</sup> seem to do better both in cross section and  $E$  and  $x_F$  dependence.

A very recent and preliminary result<sup>17</sup> by the Yale - Fermilab - LBL streamer chamber experiment appears to get a much lower cross section for hadroproduction of charm. Although in a neutron beam and at a higher energy ( $\langle E_n \rangle = 280$  GeV) their result is

$$\sigma(n+Ne-He \rightarrow D\bar{D}x) = 17 \pm 5 \pm 11 \text{ } \mu\text{b/nucleon.}$$

This group assumes an  $A^{2/3}$  dependence in calculating their result. The experiment uses a new technique under development which has very different biases from other experiments. Events with a detected  $\mu$  trigger are scanned in the streamer chamber. Tracks with angles outside 150 mr (the limit for charm decay tracks assuming central  $D\bar{D}$  production) are used to determine the primary vertex. The maximum miss distance of tracks with  $<150$  mr is plotted for  $\mu$  event (charm candidates) and non  $\mu$  events (background). There are 32  $\mu$  events and 10 ordinary events with miss distances beyond  $3\sigma$  from the primary vertex.

The CERN Hyperon group has a  $7\sigma$  narrow signal (Figure 41) in

$$\Sigma^- Be \rightarrow (\Lambda K^- \pi^+ \pi^-)x$$

This is a nice candidate for the charmed strange baryon,  $\Lambda^+(csu)$ . The  $x_F$  and  $P_T$  dependence for the signal is

$$\frac{d^3\sigma}{dP_T^2 dx_F} \sim (1-x_F)^{1.7 \pm .7} e^{-(1.1^{+.7}_{-.4})P_T^2}$$

which is reasonably similar to the distribution seen by ACCMOR. The cross section times branching ratio per nucleus for  $x > .6$  is  $\sigma_B = 5.3 \pm 2.0 \text{ } \mu\text{b/nucleus}$ . Getting a cross section per nucleon is very dependent on the  $A^\alpha$  and  $(1-x)^n$  assumptions. Table VIII shows  $\sigma_B$  for  $A^{2/3}$  and  $A$  as well as the range of  $n$  allowed by the data. This is a double charge exchange production channel which, one would think, will



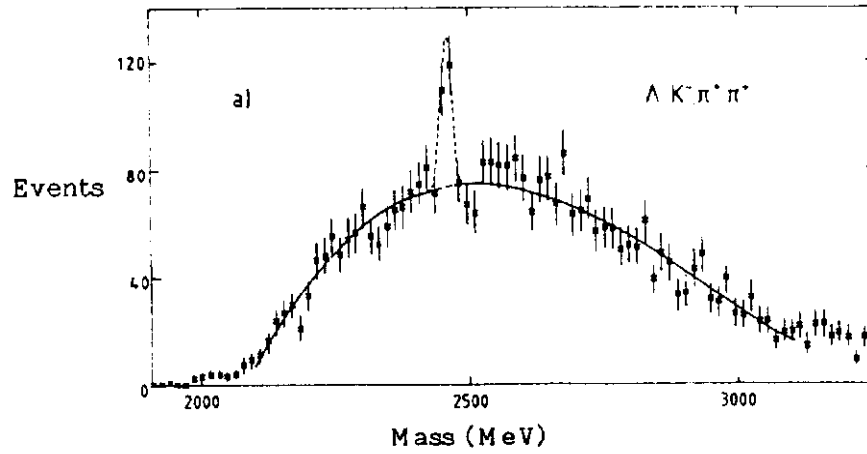


Figure 41. CERN Hyperon Experiment:  
( $\Lambda K^- \pi^+ \pi^+$ ) mass spectrum.

Table VIII

$\sigma_B$  per Nucleon of  $A^+$  Candidate for Various Assumptions

$\alpha$ $n$	$\frac{2}{3}$	1
1.0	13.3	6.4
1.7	26.4	12.7
2.4	51.8	24.9
0 for $x \leq 0.6$ 1.7 for $x > 0.6$	9.8	4.7

suppress the cross section. Nonetheless, the numbers in Table VIII are high for any reasonable branching ratio.

The experimental situation regarding cross sections in hadroproduction continues to need clarification.<sup>41</sup> A future rapporteur with more time for this subject will have plenty of grist - and some gristle - to chew on.

### CONCLUSION

I will conclude with a remark about one subject, conspicuous by its absence, that I did not talk about. Stone<sup>35</sup> reported on a 70 F signal seen by CLEO in  $e^+e^-$  production at a mass inconsistent with earlier sightings in photoproduction.<sup>42</sup> The obvious question is what do other  $e^+e^-$  and photoproduction experiments have to say on this subject. The answer, on the record at least, is "No Comment". The truth is that most (probably every) group has one or more 3, 4, or 50 F protosignals; these are at a variety of masses and in a variety of channels. They are not shown because of the general belief, which is regrettably probably correct, that if such a protosignal turns out to be a fluctuation it will tarnish the reputation of the experiment. The unfortunate result for the non specialist is an incomplete picture of the situation. I don't know what can be done about this except to report that the view from the grapevine is at least as fuzzy as that out in the open.

Luckily, as we have seen, this problem does not affect most of the other subjects in charm physics. The field is making progress slowly and steadily both in experiments and in the theoretical understanding of relevant perturbative QCD processes. Future rapporteurs will have more than they can handle in the time allowed - just as this one did.

### ACKNOWLEDGEMENTS

Quite a number of people have been very helpful in educating me about the subject in general as well as their work in particular. These include P. Avery, J.D. Bjorken, H. Burckhart, J. Butler, J. Cumalat, F. Dydak, K. Kleinknecht, C. Quigg, S. Reucroft, F. Richard, M. Shaevitz, J. Slaughter, M. Strovink, and others.

I am particularly grateful to all my colleagues on the Tagged Photon Collaboration<sup>43</sup> with whom it has been a true pleasure to work for what has been quite a large number of years. J. Spalding and K. Sliwa (who was responsible for much of the TPS D\* production analysis) were particularly helpful in the last month before Cornell. Thanks also to M. Bennett for typing this long manuscript in short order. The author's institution, Fermilab, is operated by Universities Research Associates, Inc. under contract with the U.S. Department of Energy.

## REFERENCES

- <sup>1</sup>G. Trilling, Physics Reports 75, 124 (1981).
- <sup>2</sup>Anonymous theorist, Private Communication.
- <sup>3</sup>F. Halzen, Proc. 21st Int. Conf. on High Energy Physics, (Paris 1982), J. Phys. 43, Suppl. 12, C-3, 381 (1982).
- <sup>4</sup>P. Lepage, these proceedings.
- <sup>5</sup>E. Fisk, proc. 10th Int. Symp. on Lepton and Photon Int. at High Energies (Bonn 1981), 703-729.
- <sup>6</sup>M. Strovink, *ibid*, 594-622.
- <sup>7</sup>D. Treille, *ibid*, 750-774.
- <sup>8</sup>G. Kalmus, proc. 21st Int. Conf. on High Energy Physics, (Paris 1982), J. Phys. 43, Suppl. 12, C-3, 431-469.
- <sup>9</sup>H. Abramowicz *et al.*, Z. Phys. C15, 19-31 (1982) ( $\psi$  sign dip); H. Abramowicz *et al.*, Phys. Lett. 109B, 115-118 (1982) ( $\psi$  production).
- <sup>10</sup>Y.K. Chu *et al.*, Private Communication.
- <sup>11</sup>N. Ushida *et al.*, Phys. Lett. 121B, 287-291, and 292-296 (1983).
- <sup>12</sup>A.R. Clark *et al.*, Phys. Rev. Lett. 45, 682-685 (1980); T.W. Markiewicz, Ph.D. Thesis, Berkeley, 1981 (unpublished); see also Ref. 6.
- <sup>13</sup>J.J. Aubert *et al.*, Nucl. Phys B213, 1-30 and 31-64 (1983).
- <sup>14</sup>M. Binkley *et al.*, Phys. Rev. Lett. 50, 302-305 (1983); *et al.*, Phys. Rev. Lett. 48B, 73-76 (1982).
- <sup>15</sup>S.F. Biagi *et al.*, Phys. Lett. 122B, 455-460 (1983); H.J. Burckhart, Ph.D. Thesis, Heidelberg, 1983.
- <sup>16</sup>R. Bailey *et al.*, CERN Preprints EP83-83 and 84 (1983).
- <sup>17</sup>J. Slaughter *et al.*, Private Communication.
- <sup>18</sup>A. Haatuft, K. Myklebost, J.M. Olsen, M. Willutzky, P. Petitjean, Paper C-263 submitted to this conference. (CERN-EP/83-16).
- <sup>19</sup>K. Abe *et al.*, Paper C-185 submitted to this conference and Phys. Rev. Lett. 51, 156-159 (1983); J.C. Kent, Ph.D. Thesis, Berkeley, 1983 (unpublished).
- <sup>20</sup>The NA14 Collaboration, Unnumbered paper submitted to this conference.
- <sup>21</sup>B. Denby *et al.*, Paper C-252 submitted to this conference and B. Denby, Ph.D. Thesis, Santa Barbara, 1983 (unpublished) ( $\psi$  production); K. Sliwa *et al.*, private communication ( $D^*$  production); D. Summers *et al.*, Paper C-253 submitted to this conference ( $D$  decays).
- <sup>22</sup>The following and Refs. 3, 23, 24, and 26 is a representative sample of theoretical papers on this subject: D. Duke, J. Owens, Phys. Lett. 96B, 184 (1980); J. Leveille, T. Weiler, Phys. Lett. 86B, 377 (1979) and Nucl. Phys. B147, 147 (1979); L. Jones, H. Wyld, Phys. Rev. D17, 2332 (1978); T. Weiler, Phys. Rev. Lett. 44, 304 (1980); T. Tajima, T. Watanabe, Phys. Rev. D23, 1517 (1981).
- <sup>23</sup>H. Fritzsch, Phys. Lett. 67B, 217 (1977); H. Fritzsch, K. Streng, Phys. Lett. 72B, 385 (1978).

- <sup>24</sup>E. Berger and D. Jones, Phys. Rev. D23, 1521 (1981); see also R. Baier, R. Ruckl, Bielefeld Report BI-TP 81/30 (1981).
- <sup>25</sup>P. Avery, Ph.D. Thesis, U. Illinois, 1980 (unpublished), M.S. Atiya et al., Phys. Rev. Lett. 43, 414-416 (1979) and P. Avery et al., Phys. Rev. Lett. 44, 1306-1312 (1980) (D, D\* production); J.J. Russell et al., Phys. Rev. Lett. 46, 799-802 (1981) (A production); see also B. Knapp et al., Phys. Rev. Lett. 37, 882-884 (1976).
- <sup>26</sup>J. Babcock, D. Sivers, and S. Wolfram, Phys. Rev. D18, 162-181 (1978).
- <sup>27</sup>R. Cutler, D. Sivers, Phys. Rev. D16, 679 (1977) quoted by Ref. 26.
- <sup>28</sup>J.D. Bjorken, Phys. Rev. D17, 171-173 (1978).
- <sup>29</sup>M.I. Adamovich, et al., Phys. Lett. 99B, 271 (1981); A. Fiorino et al., Lett. Nuov. Cim. 30, 166-170 (1981).
- <sup>30</sup>D. Aston et al., Phys. Lett. 94B, 113-117 (1980); see also Ref. 7 and B. D'Almagne, Proc. XX Int. Conf. High Energy Physics, Madison, 1980, AIP Proc. 68, 221-226.
- <sup>31</sup>J. Dorfan, these proceedings.
- <sup>32</sup>K. Kleinknecht and B. Renk, Z. Phys. C17, 325-328 (1983); C. Peterson, NORDITA Report 82/26, 1982 (unpublished).
- <sup>33</sup>R.E. Shrock, L.L. Wang, Phys. Rev. Lett. 41, 1692 (1978) and 42, 1589 (1979).
- <sup>34</sup>M. Shaevitz, private communication.
- <sup>35</sup>S. Stone, these proceedings.
- <sup>36</sup>Particle Data Group, Review of Particle Properties, Phys. Lett. 111B, April, 1982. Note that although there is some question about the  $D^0 \rightarrow K^- \pi^+$  branching ratio value, we have chosen to stick to the standard value for comparison purposes. Absolute values of other branching ratios dependent on this one are subject to change if, as some expect (S. Reucroft, R.J. Morrison, and others, Private Communications),  $B(K\pi)$  changes in future editions.
- <sup>37</sup>R.H. Schindler et al., Phys. Rev. D24, 78 (1981). See also Ref. 1.
- <sup>38</sup>J.L. Ritchie et al., Phys. Lett. 126B, 499-505 (1983). Phys. Lett. 113B, 77 (1982).
- <sup>39</sup>M. Crisler, private communication, to be presented by S. Childress at 9th Int. Workshop on Weak Interactions and Neutrinos, Talloires, 1983.
- <sup>40</sup>B. Combridge, Nucl. Phys. B151, 429 (1979); see also Ref. 3.
- <sup>41</sup>See Ref. 3 as well as, for example, the many useful papers in J. Tran Thanh Van and L. Montanet, eds., Moriond Workshop on New Flavours, (Ed. Frontieres, Gif - sur - Yvette, 1982).
- <sup>42</sup>D. Aston, et al., Phys. Lett. 100B, 91-94 (1981); M. Atkinson et al., Z. Phys C17, 1-4 (1983).
- <sup>43</sup>J. Bronstein, R. Morrison, D. Bintinger, U. Nauenberg, K. Daum, J. Elliott, M. Robertson, G. Luste, C. Zorn, D. Bartlett, R. Kennett, T. Nash, A. Duncan, R. Kumar, J. Spalding, A. Lu, J. Appel, D. Summers, V. Bharadwaj, A. Eisner, P. Mantsch, S. Bhadra, B. Denby,

J. Biel, K. Shahbazian, M. Streetman, J. Martin, S. Bracker,  
D. Blodgett, M. Losty, K. Stanfield, G. Kalbfleisch, K. Sliwa,  
J. Pinfold, M. Sokoloff, G. Hartner, S.E. Willis, P. Estabrooks,  
W. Schmidke, M. Witherell, S. Yellin.

## DISCUSSION

E. Paul, University of Bonn & CERN

This is a comment on observation of  $\bar{D}$  photoproduction in the WA4 experiment at the CERN Omega Spectrometer. The point is that this experiment observed  $\bar{D}$  signals with a significance around three standard deviations. These signals were improved by tagging on protons assumed to come from charmed baryon production in some fraction. In my mind this observation leaves substantial room for a contribution of  $D\bar{D}$  pair production within the range of the observed cross section.

T. Nash, Fermilab

Figure 2 in Ref. 30 shows the data that is enhanced by requiring a K or p in the WA4 experiment, which is what you are referring to. This enhancement is one of the indications of associated production. The original numbers were that  $\sigma(\bar{D}+x)$  is  $570 \pm 250$  nanobarns and  $\sigma(\Lambda_c \bar{D}+x)$  is also  $570 \pm 175$ . So what you're saying is that there is room for some pair production within those errors.

G. Wolf, DESY

You mentioned that the s/u ratio is  $\sim 0.5$  in  $\nu$  experiments while the JADE, Mark II data from  $e^+e^-$  gave  $\sim 0.3$ . The latter data come from  $K^0$  if I am not mistaken. The TASSO group looked at  $K^0$  and  $K^\pm$  production in  $e^+e^-$ . The  $K^\pm$  yield is  $\sim 60\%$  larger, the origin of which is unknown. From the  $K^\pm$  data one finds s/u  $\sim 0.5$ , from  $K^0$   $\sim 0.3$ .

T. Nash, Fermilab

I think that the SLAC TPC data is from charged K's also.

J. Wiss, University of Illinois

How does the charm system invariant mass distribution predicted by the  $\gamma g$  fusion model compare to the charm system invariant mass distribution measured by E516 for a given  $G(x)$  (gluon distribution)?

T. Nash, Fermilab

We are anxious to compare our  $M_x$  (and particularly  $M_y$ ) data with theoretical distributions but haven't seen any yet. I hope there will be gluon fusion and other calculations of these distributions available soon.

B. Roe, Michigan

There is some neutrino data giving  $\bar{s}/\bar{d} \sim .25$ . This comes from measuring  $\pi$  to K ratios on leading particles (high z) in the hadron jet in the old Fermilab E180  $\bar{\nu}$  Neon bubble chamber experiment.

Diambrini-Palazzi, Univ. of Rome-WA58

We have evidence now for a 30-35% fraction of associate production in the photon range between 20 and 70 GeV. We will present final data on photon production mechanism of charm in the next year.

T. Nash, Fermilab

Thank you. That sounds very consistent with other recent experiments.

F. Richard, Orsay

About this question of associated production. I would like to ask the speaker what he thinks about the following point. When you asked for a recoil proton to trigger your events in some sense you tend to enhance diffractive production of charm so it would be symmetrical  $D\bar{D}$ . You agree with that?

T. Nash, Fermilab

Of course, but that's not what we did for the associated production limit. The data that I referred to for that limit was from a special trigger which did not require only a single proton recoil. It required at least three tracks from the primary vertex in the recoil region and has a relatively high efficiency for  $\Lambda_c$ s in the recoil system. That trigger enhanced associated production not pair production.

C. Heusch, Univ. of Calif., Santa Cruz

You flashed by a transparency with  $\psi$  photoproduction results that demonstrated agreement with photon gluon fusion as usual, with an arbitrary scale factor. Does the measured cross section now also agree with the color singlet calculations (eg. Baier and Ruckl) that do not have that "f-factor"?

T. Nash, Fermilab

You read very quickly. The story here is that there are two types of calculations. One requires a local duality f factor. The one we are talking about is a color-singlet calculation in which you don't, in principle, have to put in an f-factor from duality.

Originally Berger and Jones did it, I believe, with a charmed mass of 1.5 GeV and the result came out about five times lower than the muon experiments. Then Baier and Ruckl redid it with a charmed mass of 1.25 GeV and that came into agreement. The point now is that the new results are really in agreement with the more traditional, more expected charm quark mass of the original Berger and Jones calculation. So it looks like the theory is in quite good shape at the moment based upon the two new photoproduction results.

C. Heusch, Univ. of Calif., Santa Cruz

Thanks. You talked something about diffractive  $D^*$  production. What did you mean by that?

T. Nash, Fermilab

What I meant by that is that the cross section results from E516 on  $D^*$  production were on  $\gamma p \rightarrow D^* x$  in the forward system plus a proton in the recoil system. That's a restrictive class of the total  $D^* X$  production and it seems to be consistent with being at least 25-30% of the total (from comparisons with the E401  $D^* x$  measurement).

C. Heusch, Univ. of Calif., Santa Cruz

Do you mean by that that the  $D^*$  is very high?

T. Nash, Fermilab

No, we have no statement on  $D^*$ . I thought I avoided using the word "diffractive" which we all tend to use loosely for elastic production as a result of our experience with vector mesons. However, the point here is that there is a cleanly identified recoiling proton and Figure 22 shows a t-shape that looks like a typical elastic channel photoproduction. It also appears the energy dependence is becoming relatively flat, though this is also the case for the total charm data. Traditionally I would call that diffractive in the Pomeron sense but that word diffractive is used in too many ways.

L. Clavelli, Argonne

Together with Cox and Holmes I have investigated another QCD subprocess to the color-singlet model for hadron-production of  $\psi$ , namely  $q\bar{q}$  to  $\psi$  gluon gluon and what we find is this dominates over the gluon gluon to  $\psi$  gluon and therefore if you add the two you will not need this anomalously high value of  $\alpha_s$  that is found in these Baier and Ruckl and Berger and Jones calculations. Applied to photoproduction this suggests that the gamma quark to  $\psi$  quark gluon will give a large contribution to this process and when one adds a few of these lowest order contributions you will saturate this process with a much lower value of  $\alpha_s$ .